Clays and Clay Minerals, Vol. 60, No. 4, 420–439, 2012.

ORGANIC GEOCHEMICAL COMPOSITION OF THE GEORGIA KAOLINS: INSIGHTS INTO FORMATION AND DIAGENETIC CONDITIONS

MICHAEL C. CHESHIRE*,‡, DAVID L. BISH, AND SIMON C. BRASSELL
Department of Geological Sciences, Indiana University, Bloomington, IN 47405, USA

Abstract—Most previous studies of the kaolin deposits in the southeastern United States have focused on their mineralogy and petrology to understand better the depositional and diagenetic environments of the kaolins. Many studies suggest, however, that much of the information held within the minerals was changed during extensive post-depositional groundwater and microbial alteration. Organic $\delta^{13}C$ and biomarker analyses were used, therefore, to provide further information on the nature of the original sediments, the depositional environment(s), and the amount of diagenetic alteration that has occurred in Georgia kaolin deposits.

Two different types of kaolin can be discerned, based on their total organic carbon contents: organic-lean kaolin and lignitic kaolin. The bulk organic $\delta^{13}C$ in the Georgia kaolins ranges from ~−26 to −19‰ (VPDB, Vienna Pee Dee Belemnite standard), with a noticeable enrichment in ^{13}C with decrease in organic carbon concentration. The lean kaolins are by far the more dominant types, with an organic-matter composition primarily of C_{16}−C_{22} *n*-alkanes, C_{16} and C_{18} fatty acids, and unresolved complex mixtures. Lignitic kaolin has a distinctly different organic matter (OM) composition. The lignitic material is primarily C_{15}−C_{33} *n*-alkanes with a greater abundance of C_{23}−C_{31} *n*-alkanes and lesser amounts of resinous and microbial constituents along with the oxidized forms of the saturated lipid fractions.

Biomarker data suggest that the lignitic material is primarily terrestrially derived from conifers with minor input from microbial lipids. The OM in both types of kaolin shows strong signs of microbial decomposition that yield the organically lean kaolins. The oxidation of the detrital organic matter would subsequently yield organic acids that would have exerted significant influence on the mineralogy and metal mobility.

Key Words—Biomarkers, Diagenesis, Geochemistry, Georgia, Hopanoids, Isotopes, Kaolinite, Lignite, Microorganisms, Organic Acids.

INTRODUCTION

Although numerous studies have addressed questions regarding the depositional environment and diagenesis of the large kaolin deposits of Georgia, USA, many uncertainties remain regarding the nature of the original sediments, the environment in which they were deposited, how much alteration took place, and how these factors influence the physical properties that make these kaolins commercially viable (White *et al.*, 1991; Dombrowski, 1993; Hurst and Pickering, 1997; Elzea Kogel *et al.*, 2002). In addition, many studies have indicated that clay-mineral surfaces have the potential to induce organic chemical reactions and to actively preserve OM (*e.g.* Brassell *et al.*, 1984; Laszlo, 1987; Kennedy *et al.*, 2002). The bulk organic $\delta^{13}C$ and OM composition of the Georgia kaolins were characterized to determine better how diagenetic alteration has influenced the kaolin deposits and to evaluate evidence of OM−kaolin interactions.

* E-mail address of corresponding author:
cheshire@lanl.gov
‡ Current address: Los Alamos National Laboratory, MS J966, Los Alamos, NM 87545, USA
DOI: 10.1346/CCMN.2012.0600408

Biomarkers

The focus of the present study was on the aliphatic and aromatic fractions. Determining the origin and degree of preservation of the organic constituents is the objective of biomarker analyses. Note that not all organic molecules can be considered as biomarkers. Biomarkers are characterized by diagnostic carbon molecular skeletons that are indicative of components from a living organism, that are common to certain organisms, and for which most of their structure is chemically stable during diagenesis (Sutton *et al.*, 2005; Peters *et al.*, 2005). Adding to the diversity of natural organic matter is the occurrence of stereoisomers and homologues of each organic constituent. Stereoisomers are different spatial arrangements of atoms or groups of molecules. In a homologous series, each member differs from the next by a $-CH_2-$ (methylene) group (Silverberg, 1996).

The primary biomarkers that are more resistant to diagenetic alteration are *n*-alkanes and terpenoids. Each of these compound classes has a specific biochemical and biophysiological role and biosynthetic pathway. *n*-Alkanes are part of an organism's mechanism for controlling diffusion of H_2O through the cell membrane (Eglinton and Hamilton, 1967). Under subaerial conditions, the organism produces higher-chained *n*-alkanes (C_{23}−C_{35}) forming waxes on the leaf surfaces, thereby

preventing desiccation. Subsurface or subaqueous organisms usually produce shorter-chain *n*-alkanes because desiccation is not a significant issue for these organisms (Killops and Killops, 2005; Peters *et al.*, 2005). Terpenoids are a broad and diverse group of organic compounds usually constructed from a series of isoprene units (C_5) forming both cyclic and acyclic constituents. Tricyclic diterpenoids are usually associated with resins of gymnosperms and are in the form of abietic and pimaric acids. Hopanes and steroids are common constituents in the cell walls of eubacteria and plants/animals, respectively.

If the preferred environment(s) for each organism and their specific biomarkers is known, biomarker analyses can provide valuable insight into specific environmental conditions that were present during sediment formation, transportation, and deposition. Understanding the conditions that lead to specific molecular alteration can lead to a better understanding of the diagenetic processes that have influenced the sediments.

Organic matter in Georgia kaolins

Previous research has shown that $\delta^{13}C$ values of organic matter in the Georgia kaolins range from −25 to −27‰ (Over *et al.*, 1987; Sprague *et al.*, 1988). Based on the isotopic data, these authors hypothesized that the Jeffersonville Mbr. clays were deposited in a brackish estuarine environment and the Buffalo Creek Fm. was deposited further inland near the limits of tidal influence. These conclusions were based on the assumption that the organic matter had remained unaltered, which implies that the $\delta^{13}C$ of organic matter has not changed from its original value. Previous studies (Hurst and Pickering, 1997; Shelobolina *et al.*, 2005), however, on the Georgia kaolins demonstrated that the organic matter has undergone extensive alteration *via* microbial and groundwater interactions. Therefore, previous conclusions based solely on organic $\delta^{13}C$ data cannot be supported and must be re-evaluated.

The lipid fraction of the organic matter in the kaolin deposits was examined by Scholefield and Whitehurst (1980) who found C_{16}−C_{38} *n*-alkanes with C_{16}−C_{28} isoprenoids, 24-ethyl-5α-cholestane, 22R- and 22S-17α(H),21β(H)-hopanes, and an unknown tetracyclic $C_{24}H_{42}$ (sesterterpene). The Scholefield and Whitehurst (1980) study failed to consider the geological significance of the organic matter distribution, however. Shelobolina *et al.* (2005) examined the water-soluble organic acids (formate, acetate, lactate, pyruvate, oxalate, and citrate). All of the lighter-weight organic acids were determined to be primary electron donors for microbial metabolisms. The Marion Mbr. kaolins had the largest total organic carbon (TOC) contents and consequently had the greatest concentrations of organic acids. Depending on the concentration of metals, organic matter, and the redox conditions, a variety of bacteria (*e.g.* Fe-reducing, Fe-oxidizing, and sulfate-reducing bacteria) can be active in the kaolin deposits (Shelobolina *et al.*, 2005, 2007). Other authors (Sutheimer *et al.*, 1999; Maurice *et al.*, 2001; Rosenberg and Maurice, 2003) discussed how organic acids and microbes could be used to remove deleterious elements from the bulk kaolin material to improve industrial processes, but they did not relate their observations to diagenetic processes.

The purpose of the present study was to investigate how the decomposition of detrital organic matter, as characterized by its carbon isotope and molecular composition, may have influenced the mineralogy of the Georgia kaolins, in addition to providing better constraints on the depositional and diagenetic environments which existed during the formation of these commercial kaolins.

SAMPLE SITES

All samples were collected from the kaolin mining district of Georgia, USA. The sedimentary kaolins were collected from open-pit mines and drill cores from Wilkinson, Washington, Glascock, McDuffie, and Jefferson Counties where extensive groundwater and microbial alteration have apparently occurred. Organic-rich kaolins have been observed further down dip from the commercial kaolin district (J. Elzea Kogel, pers. comm., 2011), but due to the depth and lack of core data, these samples were not collected and analyzed. About 0.5−1 kg of freshly exposed sedimentary kaolin was collected and wrapped in baked (500ºC/12 h) aluminum foil to minimize organic-matter contamination and stored in Hubco's (Hutchinson, Kansas, USA) 'Protexo' cloth sample bags.

ANALYTICAL METHODS

The bulk $\delta^{13}C$ composition and the TOC contents of the kaolin samples were determined using a Costech Elemental Analyzer attached to Finnigan Delta X Mass-Spectrometer. Carbon isotopic values are presented as $^{13}C/^{12}C$ ratios expressed as $\delta^{13}C$ values based on the Vienna Pee Dee Belemnite (VPDB) isotopic standard (equation 1).

$$\delta^{13}C = \frac{[^{13}C/_{12}C]_{sample} - [^{13}C/_{12}C]_{VPDB}}{[^{13}C/_{12}C]_{VPDB}} \quad (1)$$

Individual organic constituents in the kaolins were extracted *via* the Soxhlet method using a 95:5 vol./vol. dichloromethane:methanol (CH_2Cl_2:CH_3OH) solvent. The extracts were then analyzed *via* gas chromatography-mass spectrometry (GC-MS). Prior to GC-MS analyses, some samples were derivatized using pyridine and 25−50 μL N,O-bis-(trimethylsilyl)-trifluoroacetamide.

Due to the very low organic-carbon content of these kaolins, most extracts were derivatized directly and

analyzed *via* gas chromatography (GC) and/or gas chromatography/mass spectrometry (GC-MS) with no prior chromatographic separation. Some samples required silica-gel column chromatography to separate the aliphatic (F1 fraction, 10 mL hexanes) and aromatic (F2 fraction, 10 mL 2:1 CH_2Cl_2/hexanes) fractions prior to GC and GC-MS analyses, however. The extracts that did not undergo silica-gel column chromatography were typically colorless to a transparent light brown, whereas extracts that required chromatography were usually opaque, dark brown.

Routine GC analyses were run on an Agilent 6890N instrument with a flame ionization detector (FID). The GC system was operated with a cool-on-column injector and a 0.325 mm−30 m Agilent DB-5 column with He carrier. The GC column was heated from 60ºC to 320ºC at 4ºC/min and held at 320ºC for 20 (F1, saturated fraction) or 60 min (F2, aromatic fraction). GC/MS analysis was performed on an Agilent 6890N/5973 instrument, operated in splitless mode with a 0.250 mm × 30 m Restek Rtx-5Sil MS column. Helium was used as the carrier gas at 3.2 mL/min. The inlet was held at 285ºC while the column was heated from 60 to 320ºC at a heating rate of 15ºC/min and held at 320ºC for either 10 (F1, saturated fraction) or 20 min (F2, aromatic fraction). The mass spectrometer was operated under electron impact ionization conditions (70 eV) and scanned from m/z 40 to 700.

RESULTS

$\delta^{13}C$ signature

The Georgia kaolins have TOC contents ranging from 0.01 to 10 wt.% (Figures 1a, 1b) with the majority in the 0.01−0.20 wt.% range, referred to hereafter as 'lean kaolins.' The high-carbon samples (>0.2 wt.% organic C) are referred to as lignitic kaolins. Lignitic kaolins are restricted to the Marion and Jeffersonville Mbr. clays in Washington and Wilkinson Counties. No lignitic kaolins were found within the Buffalo Creek Fm.

The bulk organic $\delta^{13}C$ composition of the Georgia kaolins ranges from ~−19 to −26‰ (VPDB) (Figure 1a). Increased scatter in the $\delta^{13}C$ values with a general enrichment in ^{13}C at lower organic carbon concentrations was observed (Figure 1b). This isotopic shift suggests the presence of different organic C reservoirs with varying $\delta^{13}C$ values and that these reservoirs of organic matter are at different stages of decomposition. The Buffalo Creek Fm. kaolins tend to be more enriched in ^{13}C, with an average $\delta^{13}C$ value of −23.5‰ (σ = 1.3‰, n = 20) and are statistically indistinguishable from the Jeffersonville Mbr. kaolins, which have an average $\delta^{13}C$ of −23.8‰ (σ = 0.8‰, n = 35). The Marion Mbr. has the most ^{13}C-depleted values, with an average $\delta^{13}C$ of −24.4‰ (σ = 0.4‰, n = 16). The lignitic material, independent of age, had a $\delta^{13}C$ signature of −26.2‰ (σ = 0.7‰, n = 11).

Organic matter constituents: lignitic kaolin

Several dark brown fissile and lamellar lignitic seams, 1−2 m thick, appear to be associated with the boundary between the Marion and Jeffersonville Mbr., although to which kaolin unit they belong is unclear. The seams usually occur with a gray-tan, brittle, hard−soft kaolin with finely disseminated marcasite and pyrite. These lignitic kaolins were only observed in Wilkinson and Washington Counties and were sampled at the kin72608 and mc73108 localities. No lignitic materials were found in the eastern Georgia counties. Two samples from each locality were examined, one within the lignite (kin72608-3 and mc73108-1b) and the other from a more kaolinitic zone (kin72608-1 and mc73108-1a).

n-Alkanes. *n*-Alkanes were identified as a homologous series of components based on their m/z 85 fragment ion ($C_6H_{13}^{+*}$) responses and their molecular ions (M^+) (Brassell *et al.*, 1980; Philip, 1985). *n*-Alkanes from both lignitic lenses are dominated by larger molecular-weight compounds, ranging from C_{23} to C_{33}, with a C_{max} of C_{25} or C_{27} (Figures 2a, 3a). The odd-to-even preference (C_{23}−C_{33}) is variable, with a carbon preference index (CPI, equation 2) ranging from 1.37 to 2.77, suggesting that these lignitic phases probably contain OM derived from a combination of different plant sources with varying degrees of diagenetic maturity (Table 1). The higher homologues are characteristic of epicuticular waxes typical of terrestrial higher plants (Eglinton and Hamilton, 1967), whereas the lower homologues (<C_{21}) typically originate from phytoplankton or microorganisms.

$$\mathrm{CPI} = \left[\left[\frac{(C_{25}+C_{27}+C_{29}+C_{31}+C_{33})}{(C_{26}+C_{28}+C_{30}+C_{32}+C_{34})}\right] + \left[\frac{(C_{25}+C_{27}+C_{29}+C_{31}+C_{33})}{(C_{24}+C_{26}+C_{28}+C_{30}+C_{32})}\right]\right] \times \frac{1}{2} \quad (2)$$

Cyclic terpanes. Terpenoids were identified from their m/z 191 fragment ion responses associated with their comparative GC retention times and characteristic MS fragmentation patterns (Seifert and Moldowan, 1978; Brassell *et al.*, 1980; Philps, 1985). Additional sources of spectral and chromatographic data were used to identify diterpanes (Blunt *et al.*, 1988; Killops *et al.*, 1995; Otto *et al.*, 1997; Peters *et al.*, 2005). The terpanes consist of a series of sesquiterpanes, tricyclic diterpanes, tetracyclic terpanes, and pentacyclic terpanes (Figure 4). Each hopane homologue occurs in 17α(H),21β(H); 17β(H),21α(H); and 17β(H),21β(H) stereochemistries; which are the dominant configurations in geological materials.

Lignite from kin72608-1 and kin72608-3 contained only the hopane homologues (Figure 2b), whereas the lignite seam from mc73108-1a and mc73108-1b contained all types of terpanes observed in this study (Figure 3b). Cadalene was the only sesquiterpene

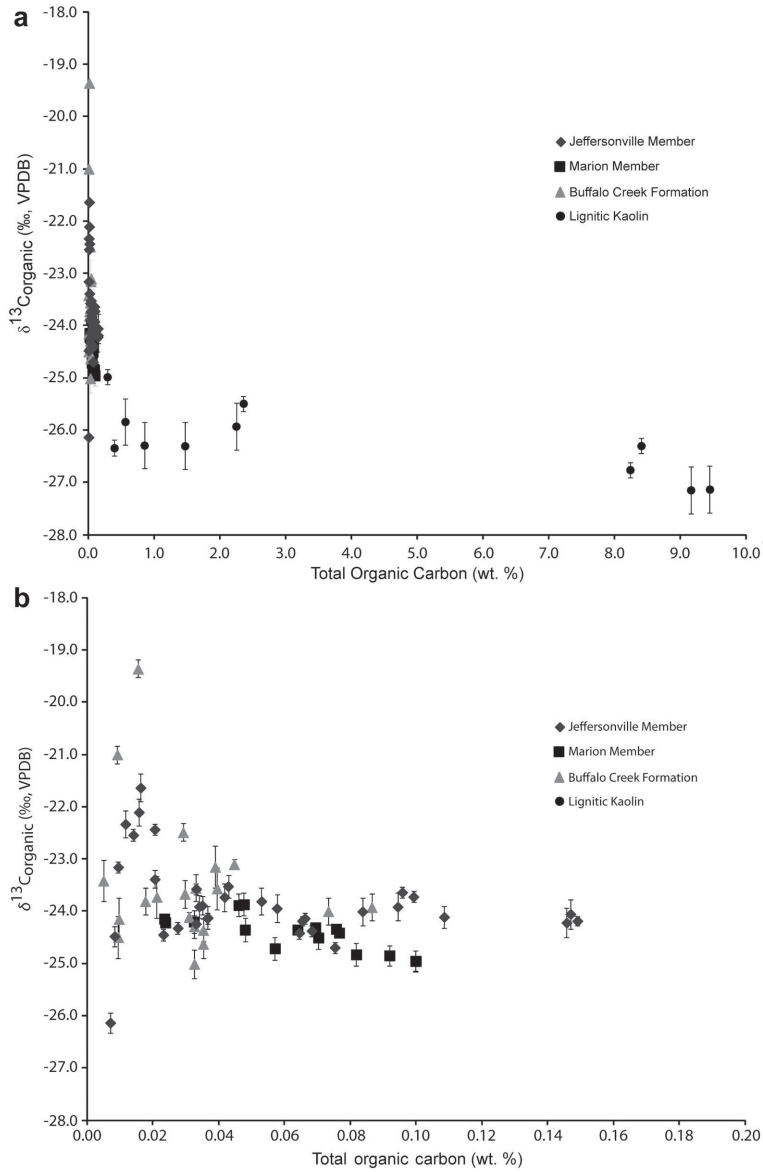

Figure 1. Relationship between $\delta^{13}C$ and total organic carbon (TOC) contents of different kaolin units: (a) all kaolin samples; (b) lean kaolins with TOC contents <0.2 wt.%.

observed in the lignites studied (Figure 4j). Norisopimarane (Figure 4k) and sandaracopimarane (isoprimarane; Figure 4l) are the major diterpanes in the mc73108 lignite, with sandaracopimarane forming ~85.7% of the total sesquiterpenes. Tetracyclic terpanes from the mc73108 lignite comprise C_{24}–C_{26} 17,21-secohopane homologues (Figure 4m, n, and o). The C_{26} homologue is the dominant 17,21-secohopane constituent (56.6%) with C_{25} and C_{24} homologues present in lesser amounts (34.0% and 9.4%, respectively). The carbon number distribution of hopanes is summarized in Table 2. The hopane series ranges from the 17α(H) and 17β(H) 22,29,30-trisnorhopanes (Ts and Tm, $C_{27}H_{46}$) to 17α(H),21β(H) and 17β(H),21α(H) 22R bishomohopanes ($C_{32}H_{56}$) with the exception of 28,30-bisnorhopanes ($C_{28}H_{48}$), which are not present in the lignites (Figures 4, 1–13). The dominant stereoisomers in both lignites were 17α(H),21β(H)-hopanes (αβ) and 17β(H),21α(H)-hopane (βα) homologues, with lesser amounts of 17β(H),21β(H)-hopane (ββ). The hopane distributions provide a measure of the maturity of the samples based on the proportions of the various stereoisomers (αβ *vs*. βα *vs*. ββ) and the Ts/(Ts+Tm) ratio, which reflects the greater resistance of Ts (17α(H)-22,29,30-trisnorhopane) to thermal degradation relative to Tm (17β(H)-22,29,30-trisnorhopane). The values for Ts/(Ts+Tm) are 0.189 and 0.152 for the kin72608-3 and mc73108-1b lignites, respectively.

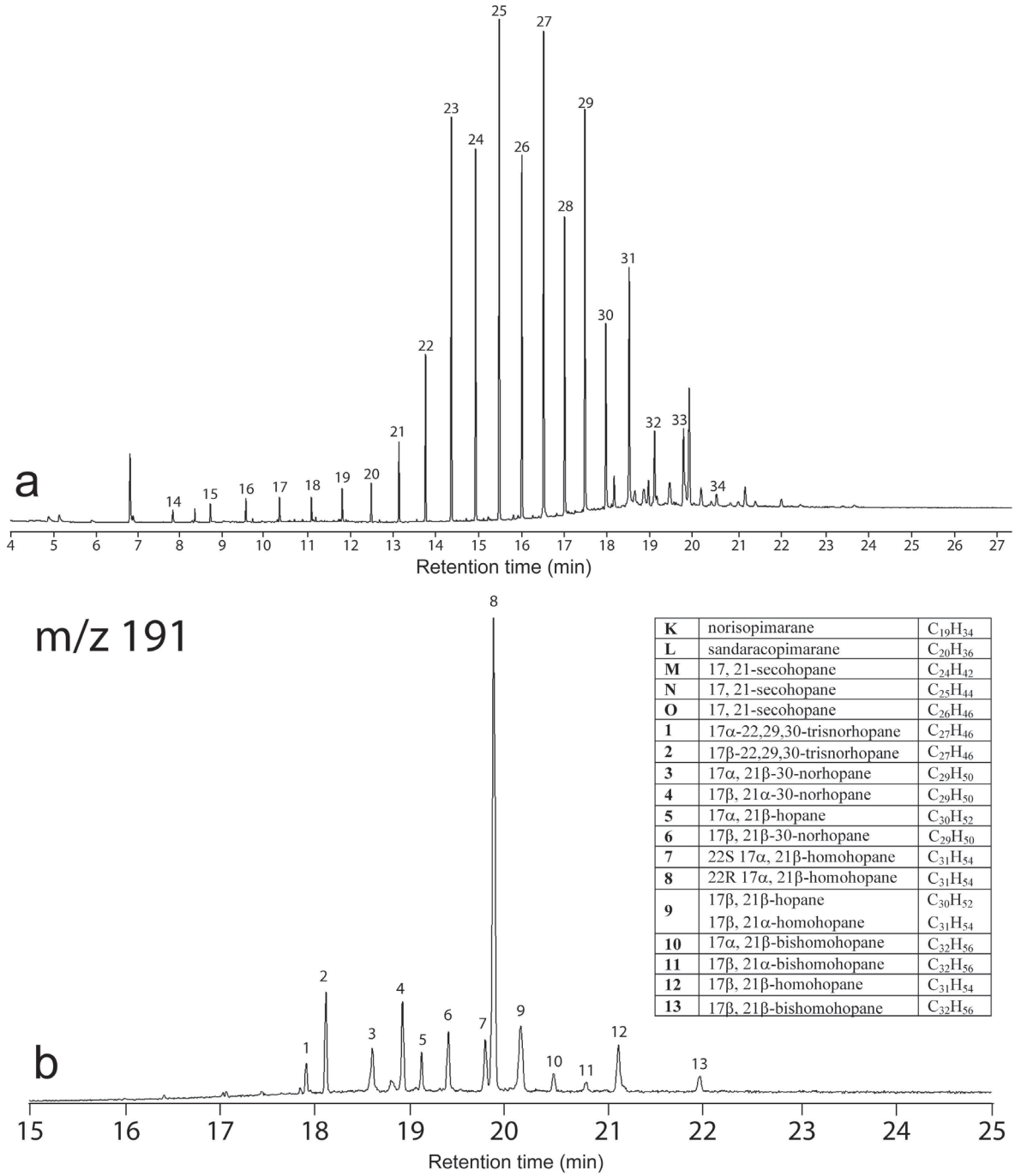

Figure 2. GC-MS data from the kin72608-3 F1 fraction: (a) total ion chromatograph showing the *n*-alkane distribution. The numbers at each peak represent the C numbers. (b) The m/z 191 fragmentogram showing the terpenoid species.

Oxygenated-alkyl constituents. The major constituents of the 'aromatic' fractions (F2) are *n*-alkyl ketones (*n*-alkanones) and aldehydes (*n*-alkanals) (Figure 5a,b). Other oxygenated constituents present in the lignites include diketones (*n*-alkandiones), methyl esters (methyl alkenoates), and various oxygenated cyclic terpenoids. The series of *n*-alkanones were identified in m/z 58/59 (*n*-alkan-2-ones), m/z 72 (*n*-alkan-3-ones), and m/z 86 m/z (*n*-alkan-4-ones) mass fragmentograms aided by evidence from their relative retention times and other characteristics of their mass spectra as described by Leif and Simoneit (1995) (Figures 6a, 7a). Four types of *n*-alkanones are present in the lignites: *n*-alkan-2-ones, *n*-alkan-3-ones, *n*-alkan-4-ones, and *n*-alkan-2,5-diones (Figure 8), with *n*-alkan-2-one and *n*-alkandione homologues as the dominant ketone constituents.

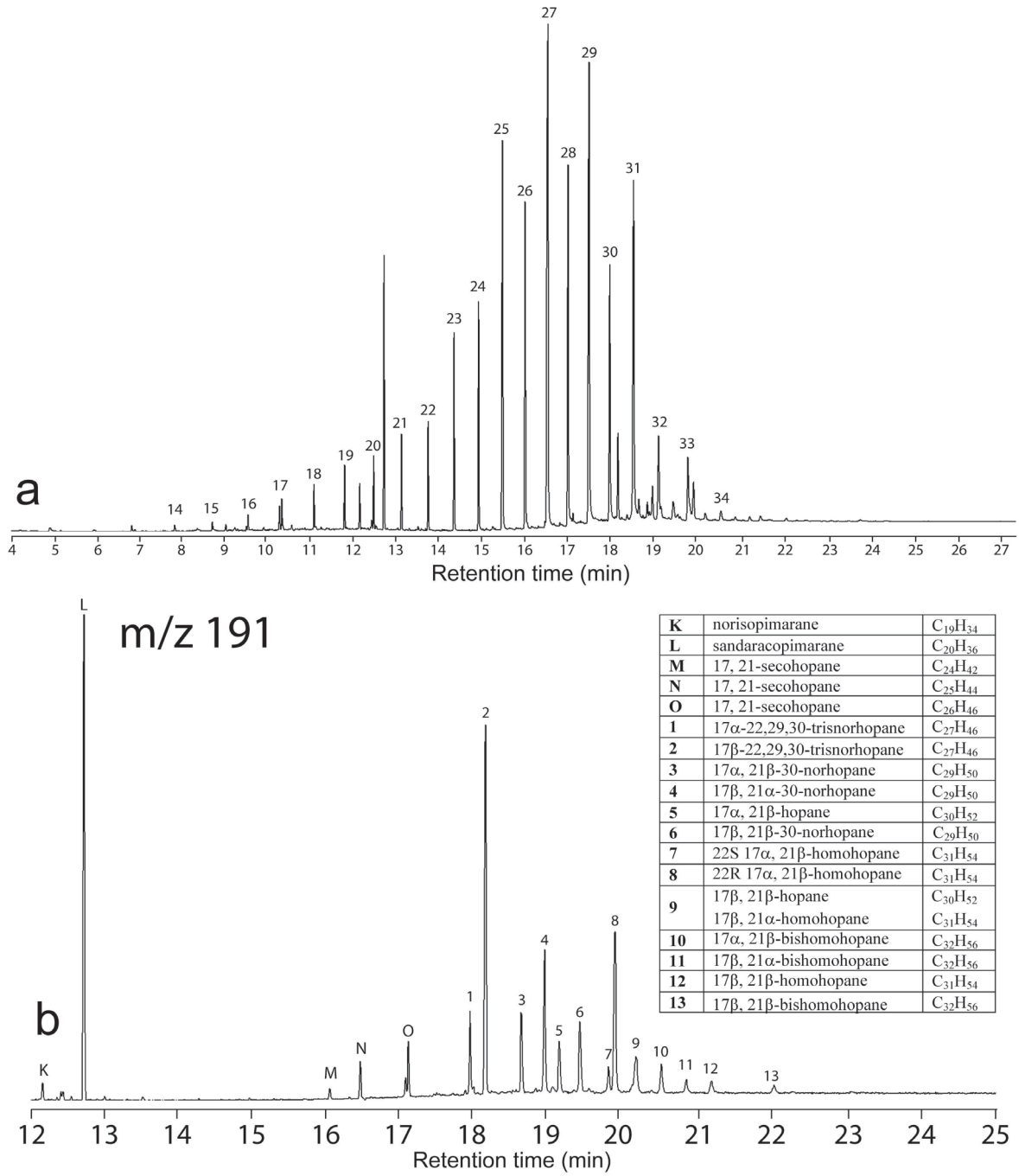

K	norisopimarane	$C_{19}H_{34}$
L	sandaracopimarane	$C_{20}H_{36}$
M	17, 21-secohopane	$C_{24}H_{42}$
N	17, 21-secohopane	$C_{25}H_{44}$
O	17, 21-secohopane	$C_{26}H_{46}$
1	17α-22,29,30-trisnorhopane	$C_{27}H_{46}$
2	17β-22,29,30-trisnorhopane	$C_{27}H_{46}$
3	17α, 21β-30-norhopane	$C_{29}H_{50}$
4	17β, 21α-30-norhopane	$C_{29}H_{50}$
5	17α, 21β-hopane	$C_{30}H_{52}$
6	17β, 21β-30-norhopane	$C_{29}H_{50}$
7	22S 17α, 21β-homohopane	$C_{31}H_{54}$
8	22R 17α, 21β-homohopane	$C_{31}H_{54}$
9	17β, 21β-hopane 17β, 21α-homohopane	$C_{30}H_{52}$ $C_{31}H_{54}$
10	17α, 21β-bishomohopane	$C_{32}H_{56}$
11	17β, 21α-bishomohopane	$C_{32}H_{56}$
12	17β, 21β-homohopane	$C_{31}H_{54}$
13	17β, 21β-bishomohopane	$C_{32}H_{56}$

Figure 3. GC-MS data from the mc73108-1b F1 fraction: (a) total ion chromatograph showing the *n*-alkane distribution. The numbers at each peak represent the C. (b) The m/z 191 fragmentogram showing the terpenoid species.

n-Alkan-2-ones range from $C_{12}H_{24}O$ to $C_{35}H_{70}O$, with a C_{max} of C_{27}, a dominance of odd homologues, and CPI values of 1.45–1.54 (Table 1). *n*-Alkandiones range from $C_{21}H_{40}O_2$ to $C_{33}H_{64}O_2$ with a C_{max} of C_{28}, a dominance of even homologues and CPI values of 1.26–1.70 (Table 1). The kin72608 lignite contains a greater concentration of *n*-alkan-3-ones and *n*-alkan-4-ones compared with the mc73108 lignite (Figure 9a,b).

The *n*-alkanals were identified in the kin72608 lignite from their characteristic m/z 82 mass fragment (Figure 5) and the $[M\text{-}18]^{+*}$ ion generated by loss of H_2O associated with the carbonyl at the α-C position. The *n*-alkanals range from $C_{12}H_{24}O$ to $C_{29}H_{58}O$, with a C_{max} of C_{24} or C_{26}, a dominance of even homologues, and CPI values of 1.21–1.47 (Table 1, Figure 9a). They were not detected in the mc73108 lignite (Table 1, Figure 6).

Table 1. Alkyl lipid classes associated with lignites from samples kin72608 and mc73108. Samples kin72608-3 and mc73108-1b represent the lignites themselves, whereas samples kin72608-1 and mc73108-1a derive from the more kaolinitic zone (O-E = odd/even; E-O = even/odd; b.d.l. = below detection limits).

	kin72608-1				kin72608-3			
	C range	C_{max}	CPI	C_{pref}	C range	C_{max}	CPI	C_{pref}
n-alkanes	13–34	27	1.37	O-E	11–35	25	1.59	O-E
n-alkan-2-ones	12–33	27	1.45	O-E	13–35	27	1.49	O-E
n-alkan-3-ones	21–31	29	0.79	O-E	15–31	26	b.d.l.	O-E
n-alkan-4-ones	27–29	28	b.d.l.	b.d.l.	24–29	26	b.d.l.	b.d.l.
n-alkanals	12–29	26	1.47	E-O	12–29	24	1.21	E-O
n-alkandiones	23–33	28	1.26	E-O	22–33	28	1.27	E-O
n-alkanoates	22–29	26	b.d.l.	b.d.l.	22–29	26	b.d.l.	b.d.l.

	mc73108-1a				mc73108-1b			
	C range	C_{max}	CPI	C_{pref}	C range	C_{max}	CPI	C_{pref}
n-alkanes	14–33	27	2.77	O-E	11–35	27	1.93	O-E
n-alkan-2-ones	22–29	27	b.d.l.	O-E	15–33	27	1.54	O-E
n-alkan-3-ones	27	b.d.l.	b.d.l.	b.d.l.	22–29	27	b.d.l.	O-E
n-alkan-4-ones	b.d.l.	b.d.l.	b.d.l.	b.d.l.	23–29	27	b.d.l.	O-E
n-alkanals	b.d.l.	b.d.l.	b.d.l.	b.d.l.	16–28	b.d.l.	b.d.l.	b.d.l.
n-alkandiones	25–27	27	b.d.l.	E-O	21–32	28	1.70	E-O
n-alkanoates	23–29	28	b.d.l.	b.d.l.	19–29	28	1.40	E-O

Organic-matter constituents: organically lean kaolin

Organic geochemical data from the lean kaolins are summarized in Tables 3, 4, and 5. The lean kaolins primarily contain unresolved complex mixtures (UCM), which have been described as a mixture of linear hydrocarbon chains connected at one or more branch points and which are typically resistant to biodegradation (Peters *et al.*, 2005). The UCM hump in the kaolin samples elutes at about the same time as the C_{15} to C_{22} *n*-alkanes (Figure 9). Minor organic constituents in the lean kaolins include *n*-alkanes, C_{16}– and C_{18}-fatty acids, polyaromatic compounds (PAH, *e.g.* phenanthrene), and elemental sulfur. Humic materials and asphaltenes appear to be present in the extracts but were removed prior to GC-MS analyses and were, therefore, not characterized. The *n*-alkanes are primarily in the range C_{16}–C_{23}, with a C_{max} typically of ~C_{17} or C_{18}.

Due to the observed distribution of chain lengths in the lean kaolins, a traditional carbon preference index (CPI, equation 2) could not be calculated for most samples. Instead, even-to-odd chain-length ratios were calculated, maintaining an equal number of data points for each even/odd calculation and centering on the C_{max}. The even/odd ratio for the most-lean kaolins ranged from 0.80 to 1.00, suggesting that most samples have no strong preference for either even or odd carbon numbers. Fatty acids present in the lean kaolins are *n*-hexadecanoic ($CH_3(CH_2)_{14}COOH$) and *n*-octadecanoic ($CH_3(CH_2)_{16}COOH$) acids. These acids appear to be more dominant in the Wilkinson and Washington County kaolins and are associated with kaolin units containing iron sulfide minerals. Organic matter observed in the lean samples is consistent throughout the various localities, regardless of age or stratigraphic position.

Three samples displayed a broader range of *n*-alkanes. Sample cs72508-8 has a unimodal chain-length distribution ranging from C_{17} to C_{31} with a C_{max} at C_{23} (Figure 10). Essentially no odd or even carbon length preference with an even/odd ratio of 1.03 exists. Sample enn71908-3 displays a bimodal *n*-alkane distribution with

Table 2. Relative abundances of hopane homologues from lignite samples mc73108 and kin72608. $C_n = I_{Cn}/(I_{C27}+I_{C28}+I_{C29}+I_{C30}+I_{C31}+I_{C32})$; I_{Cn} = integrated intensity from GC plot; *n* = carbon number of specific hopane; n.d.= not detected.

Hopane homologues	$C_{27}H_{46}$	$C_{28}H_{48}$	$C_{29}H_{50}$	$C_{30}H_{52}$	$C_{31}H_{54}$	$C_{32}H_{56}$
mc73108-1a	0.451	n.d.	0.332	0.030	0.187	0.000
mc73108-1b	0.404	n.d.	0.255	0.039	0.235	0.066
kin72608-1	0.157	n.d.	0.223	0.027	0.473	0.120
kin72608-3	0.107	n.d.	0.108	0.077	0.594	0.059

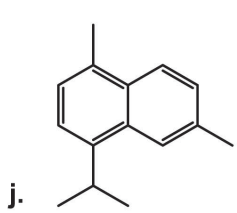

j. cadalene ($C_{15}H_{18}$)

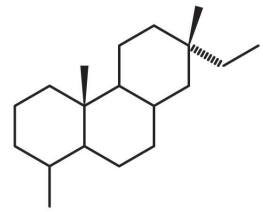

k. 18-norisopimarane ($C_{19}H_{34}$)

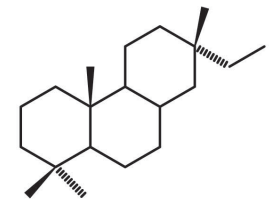

l. sandaracopimarane ($C_{20}H_{36}$) (a.k.a., isopimarane)

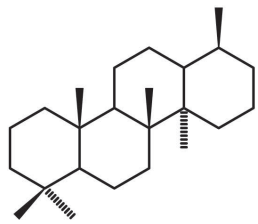

m. 17,21-secohopane ($C_{24}H_{42}$)

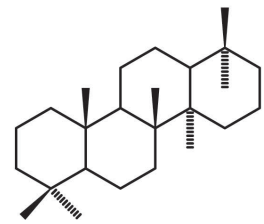

n. 17,21-secohopane ($C_{25}H_{44}$)

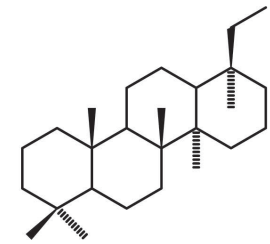

o. 17,21-secohopane ($C_{26}H_{46}$)

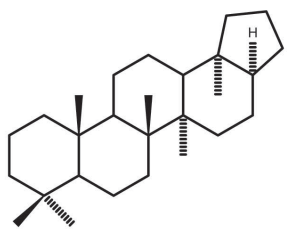

1. 17α(H)-22,29,30-trisnorhopane (Ts, $C_{27}H_{46}$)

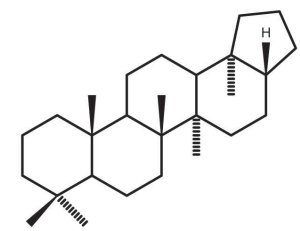

2. 17β(H)-22,29,30-trisnorhopane (Tm, $C_{27}H_{46}$)

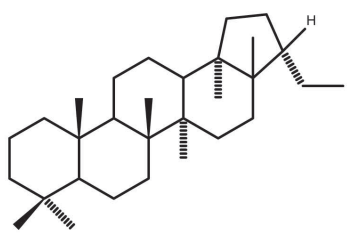

3, 4, 6. 17α(H),21β(H); 17β(H),21α(H); 17β(H),21β(H)–30–norhopane ($C_{29}H_{50}$)

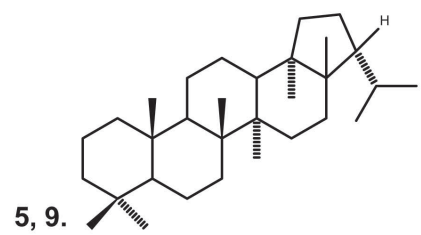

5, 9. 17α(H),21β(H);17β(H),21α(H)-hopane ($C_{30}H_{52}$)

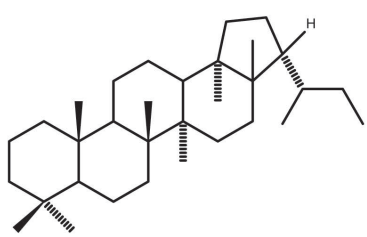

7-9, 12. **22S**, **22R** 17α(H),21β(H); 17β(H),21α(H); 17β(H),21β(H)-homohopane ($C_{31}H_{54}$)

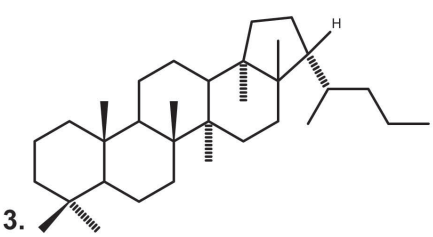

10, 11, 13. 17α(H),21β(H); 17β(H),21α(H); 17β(H),21β(H)-bishomohopane ($C_{32}H_{56}$)

Figure 4. Structures of terpenoid series identified by GC-MS analyses (m/z 191 fragmentograms).

chain-length range from C_{16} to C_{27}, with a C_{max} at C_{18} and C_{23} (Figure 11). This sample does not display an odd or even carbon length preference, with an even/odd ratio of 1.04. The other sample displaying a bimodal *n*-alkane

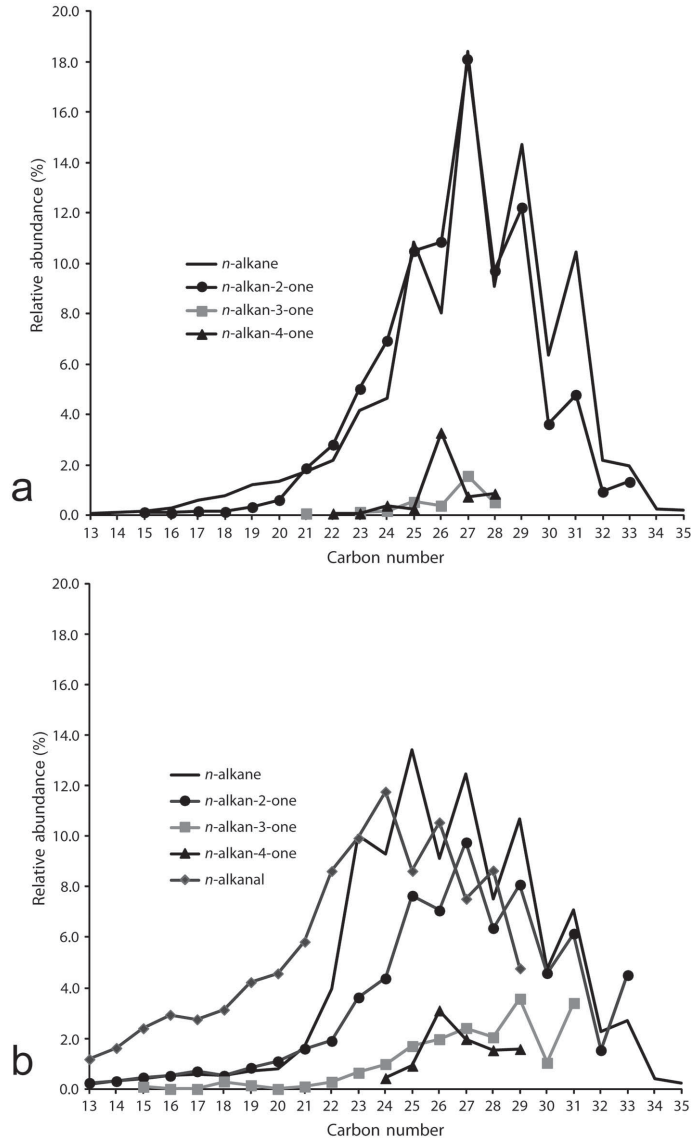

Figure 5. Graphs showing the relative abundance and carbon number distribution of the *n*-alkanes, *n*-alkanones, and *n*-alkanals homologues. Each series is normalized to their cumulative integrated peak intensities. (a) kin72608-3 and (b) mc73108-1b.

distribution is also from Washington County (rou62608-4) (Figure 12). The *n*-alkanes in this sample have a carbon chain length ranging from C_{16} to C_{34}, with a C_{max} at C_{17} and C_{29}. The lighter-weight *n*-alkanes ($C_{16}-C_{22}$) have an odd carbon length preference (even/odd = 0.69), and a moderate odd-over-even preference was present within the long-chain *n*-alkanes ($C_{23}-C_{29}$) (CPI = 1.81).

DISCUSSION

$\delta^{13}C$ composition

The organic $\delta^{13}C$ data from the kaolins are indicative of C_3-type higher plant constituents, and the $\delta^{13}C$ values often range from −22 to −34‰ (Vogel, 1993). The carbon mass-dependent isotopic fractionations observed for C_3-plants are primarily due to CO_2 diffusion into the cells and the carboxylation of the ribulose bisphosphate carboxylase (O'Leary, 1981, 1993). C_3-plant dominance is typical for pre-Miocene plant material because C_4-plants did not become a significant organic matter contributor until the late Miocene period (Zachos *et al.*, 2001). Apparently microbial and/or algal organic matter contributed to the total organic matter composition, but did not significantly alter the bulk isotopic values. The organic geochemical data support the domination of terrestrial higher plants and bacterial lipids in the extractable organic matter in the kaolin deposits. Apparently, microbial lipids are currently the dominant form of organic matter in the lean kaolins, whereas terrestrial plant matter was the primary source of organic matter during deposition.

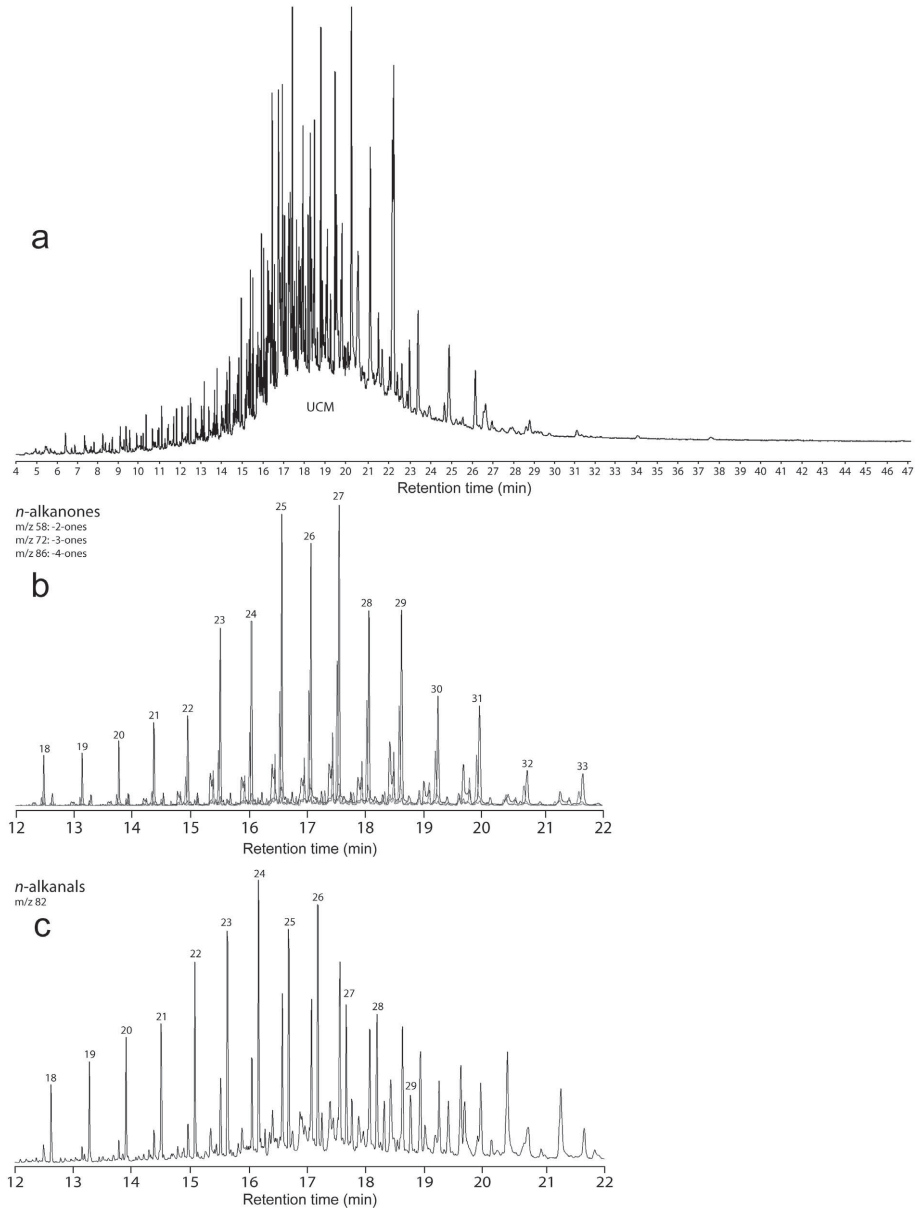

Figure 6. GC-MS data from the kin72608 lignite located in Wilkinson County: (a) total ion chromatograph of the 'aromatic' fraction; (b) mass fragmentographs showing the *n*-alkan-2-one (m/z 58), *n*-alkan-3-one (m/z 72), and *n*-alkan-4-one (m/z 86) distributions; and (c) fragmentographs showing the *n*-alkanal (m/z 82) distribution. Peak designations refer to constituent carbon numbers. UCM = unresolved complex mixture.

Plant matter consists of a complex mixture of cellulose and lignin comprising ~90 dry wt.% of the plant, with lesser amounts of lipids, carbohydrates, and amino acids. Each component tends to have different $\delta^{13}C$ values, ranging from −27‰ (lignin) to −23‰ (cellulose) for C_3 plants (Benner *et al.*, 1987). Compositional variations are the primary factors determining $\delta^{13}C$ fractionation during decomposition. Cellulosic material tends to decay at a much faster rate than lignin (Benner *et al.*, 1987). As plant matter decomposes, it retains a greater concentration of lignin and subsequently becomes more depleted in ^{13}C (*i.e.* negative $\delta^{13}C$ excursion). This trend was not observed in the $\delta^{13}C$ data collected from the Georgia kaolins, however. Instead, enrichment of ^{13}C (*i.e.* positive $\delta^{13}C$ excursion) occurred as the organic carbon concentration decreased. The positive $\delta^{13}C$ excursion related to organic carbon concentrations resembles the signature derived from microbial decomposition of organic matter. Enrichment of ^{13}C during biodegradation occurred due to the preferential cleavage of the weaker $^{12}C-^{12}C$ bonds compared with stronger $^{13}C-^{13}C$ or $^{12}C-^{13}C$ bonds (Faure and Mensing, 2005).

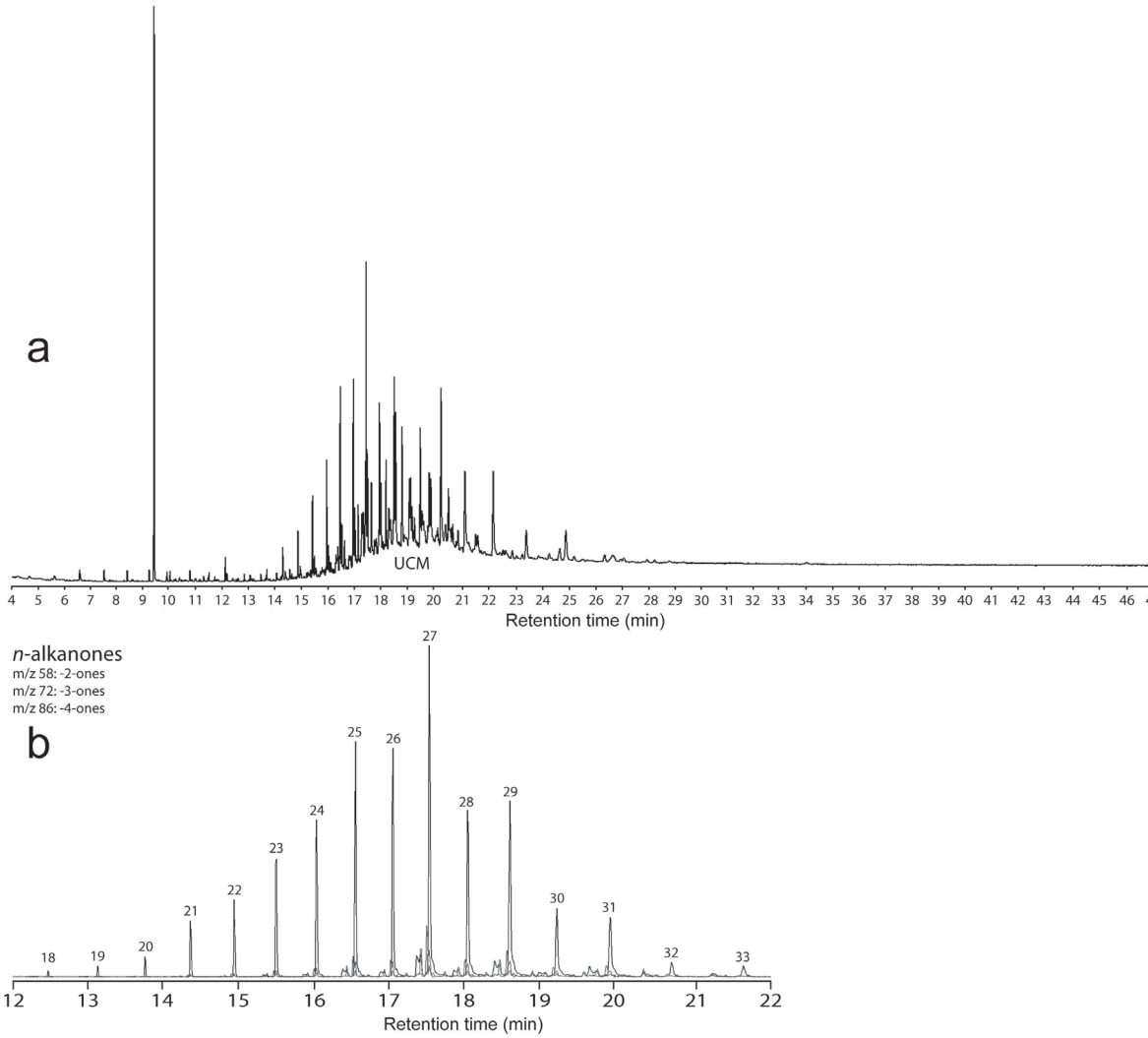

Figure 7. GC-MS data from the mc73108 lignite located in Washington County: (a) total ion chromatograph of the 'aromatic' fraction; and (b) fragmentographs showing the *n*-alkan-2-one (m/z 58), *n*-alkan-3-one (m/z 72), and *n*-alkan-4-one (m/z 86) distributions. Peak designations refer to constituent carbon numbers. UCM = unresolved complex mixture.

Lignitic kaolin

Organic matter in the lignitic kaolins appears to be primarily terrestrially derived from vascular C_3 plant material, probably from a conifer-based ecology, with a significant contribution from peats associated with the depositional locality. The lignitic kaolins may have resulted from local depositional changes that allowed the accumulation of peat and organic matter detritus,

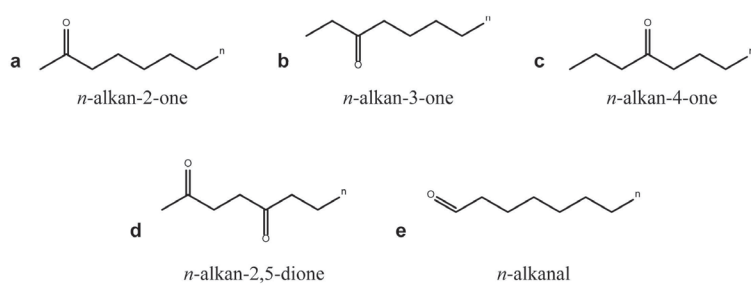

Figure 8. Oxygenated *n*-alkyl constituents isolated from the lignitic kaolins. '*n*' attached to the molecular structures represents a variety of lengths for *n*-alkyl chains that constitute the homologous series of the alkanones and alkanals.

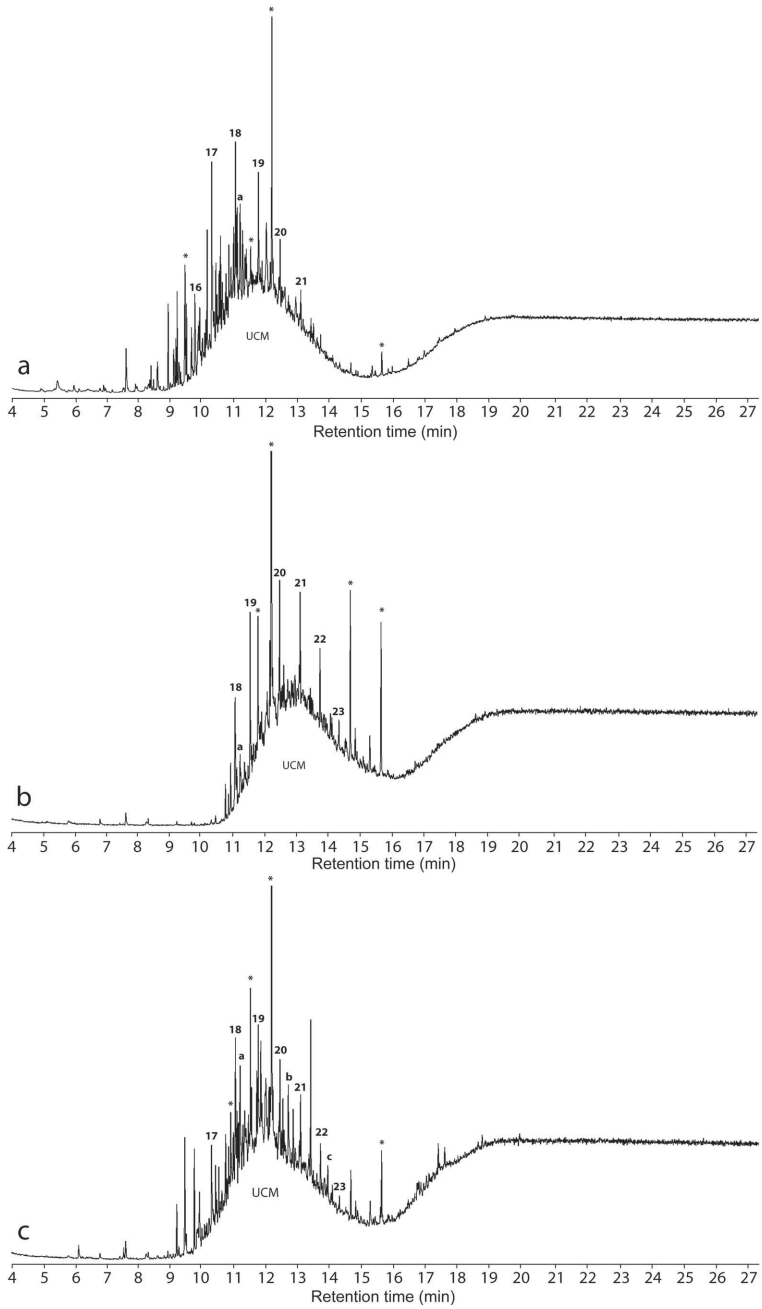

Figure 9. Total ion chromatographs of (a) hob80808-6 (Glascock County); (b) doc62808-3 (Washington County); and (c) kc71208-4 (Wilkinson County) extracts. Peak numbers represent the carbon number for each *n*-alkane. UCM = unresolved complex mixture. * represents phthalate and silicone contamination.

followed by a shift back to a clastic or clay-dominated depositional environment. Peat accumulation requires a delicate balance between depositional rate, peat accumulation rate, and decay rate, all of which are related to climatic conditions. In tropical regions, peat accumulation is associated with very high rainfall, causing a water-logged and subsequently anoxic depositional environment (Killops and Killops, 2005). Peats can also form in paralic environments where sediment fluxes have been reduced by bars, spits, or levees (Killops and Killops, 2005).

The *n*-alkane distribution and odd-over-even predominance in the lignite are typical for epicuticular waxes (Eglinton and Hamilton, 1967). The distribution centered on the $C_{27}H_{54}$ *n*-alkane is characteristic of a warm-humid terrestrial environment because the long-chain

Table 3. Relative abundances of *n*-alkane homologues and organic signatures of lean kaolins from the eastern counties of the kaolin district.

	ccc72508-2	cs72508-6	hob80808-6
C_{16}	b.d.l.	b.d.l.	0.281
C_{17}	b.d.l.	0.090	1.000
C_{18}	0.577	0.336	0.632
C_{19}	1.000	0.510	0.275
C_{20}	0.457	0.564	0.190
C_{21}	0.126	0.545	0.117
C_{22}	0.059	0.847	0.044
C_{23}	0.063	1.000	0.013
C_{24}	b.d.l.	0.878	0.009
C_{25}	b.d.l.	0.580	0.013
C_{26}	b.d.l.	0.411	0.017
C_{27}	b.d.l.	0.350	0.025
C_{28}	b.d.l.	0.275	0.020
C_{29}	b.d.l.	0.249	0.017
C_{30}	b.d.l.	0.104	b.d.l.
C_{31}	b.d.l.	0.057	b.d.l.
C_{range}	18−23	17−31	16−29
C_{max}	19	23	17
Even/Odd	0.92	1.03	0.82
Pr/Ph	b.d.l.	b.d.l.	0.58
TOC (wt.%)	0.012	0.018	0.010
$\delta^{13}C$ (‰)	n.d.	n.d.	n.d.

b.d.l. = below detection limits, n.d. = not determined.

n-alkanes (waxes) help to control H_2O vapor diffusion into and out of the leaf surface (Eglinton and Hamilton, 1967). The uniform C_{max} for all lignite samples in this study suggests that major climate shifts experienced during the Paleocene and Eocene periods did not significantly affect the ecology. The CPIs of the *n*-alkanes are usually a good indication of the maturity of organic matter. Vascularized terrestrial plants have a very high CPI, usually $\geqslant 3.0$ (Eglinton and Hamilton, 1967; Hostettler *et al.*, 1989). During maturation, the CPI of the *n*-alkanes approaches 1.0, due to random cleavage of alkyl-chains, producing *n*-alkanes with no odd or even predominance (Killops and Killops, 2005). The CPI range of 1.37−2.77 for the lignites indicates that their organic matter is of an increased maturity. In most organic geochemical studies, an increase in maturity refers to increased pressure or temperature as a result of burial (Killops and Killops, 2005). However, these kaolins have not experienced deep burial or compaction, as indicated by the lack of bedding planes and random particle orientations (data not presented). In addition, Hassanipak and Eslinger (1985) showed, *via* kaolinite δ^2H and $\delta^{18}O$ compositions, that the kaolin deposits formed within a temperature range of 20−35ºC, well below the temperatures required for thermally induced organic-matter maturation. Therefore, a more likely source for the observed increase in *n*-alkane maturity is microbial biodegradation.

Table 4. Relative abundances of *n*-alkane homologues and organic signatures of lean kaolins from Washington County.

	che62608-6	rou62608-4	enn71908-3	doc62608-3	mc73108-2a
C_{16}	b.d.l.	0.165	0.100	b.d.l.	0.087
C_{17}	b.d.l.	0.600	0.552	b.d.l.	0.863
C_{18}	0.812	0.364	1.000	0.622	1.000
C_{19}	1.000	0.219	0.645	1.000	0.501
C_{20}	0.747	0.157	0.531	0.899	0.425
C_{21}	0.477	0.147	0.545	0.806	0.400
C_{22}	0.154	0.142	0.818	0.149	0.157
C_{23}	0.092	0.193	0.968	b.d.l.	0.030
C_{24}	b.d.l.	0.175	0.725	b.d.l.	b.d.l.
C_{25}	b.d.l.	0.524	0.405	b.d.l.	b.d.l.
C_{26}	b.d.l.	0.335	0.170	b.d.l.	b.d.l.
C_{27}	b.d.l.	0.657	0.070	b.d.l.	b.d.l.
C_{28}	b.d.l.	0.385	b.d.l.	b.d.l.	b.d.l.
C_{29}	b.d.l.	1.000	b.d.l.	b.d.l.	b.d.l.
C_{30}	b.d.l.	0.637	b.d.l.	b.d.l.	b.d.l.
C_{31}	b.d.l.	0.668	b.d.l.	b.d.l.	b.d.l.
C_{32}	b.d.l.	0.209	b.d.l.	b.d.l.	b.d.l.
C_{33}	b.d.l.	0.410	b.d.l.	b.d.l.	b.d.l.
C_{34}	b.d.l.	0.111	b.d.l.	b.d.l.	b.d.l.
C_{range}	18−23	6−34	16−27	18−23	16−23
C_{max}	19	17/29	18/23	19	18
Even/Odd	1.09	0.69	1.04	0.84	0.90
Pr/Ph	b.d.l.	b.d.l.	0.46	b.d.l.	b.d.l.
TOC (wt.%)	0.012	0.053	0.017	0.039	0.064
$\delta^{13}C$ (‰)	−22.3(3)	−23.8(3)	n.d.	−23.2(4)	−24.4(2)

b.d.l. = below detection limits, n.d. = not determined.

Table 5. Relative abundances of *n*-alkane homologues and organic signatures of lean kaolins from Wilkinson County.

	blo72608-2	kc71208-2	kc71208-4	mc71708-2a	mc71708-5a
C_{16}	b.d.l.	b.d.l.	0.070	0.260	0.219
C_{17}	b.d.l.	0.236	0.667	1.000	0.648
C_{18}	0.518	1.000	1.000	0.691	1.000
C_{19}	1.000	0.905	0.411	0.335	0.264
C_{20}	0.911	0.836	0.335	0.279	0.228
C_{21}	0.801	0.768	0.260	0.223	0.201
C_{22}	0.843	0.497	0.163	0.124	0.121
C_{23}	0.591	0.192	0.050	0.040	0.047
C_{24}	0.258	b.d.l.	b.d.l.	b.d.l.	b.d.l.
C_{25}	0.109	b.d.l.	b.d.l.	b.d.l.	b.d.l.
C_{range}	18–25	17–23	16–23	16–23	16–23
C_{max}	19	18	18	17	18
Even/Odd	0.95	1.22	1.12	0.70	1.21
Pr/Ph	b.d.l.	b.d.l.	b.d.l.	0.76	b.d.l.
TOC (wt.%)	0.043	0.031	0.065	0.030	0.099
$\delta^{13}C$ (‰)	n.d.	−23.9(2)	−24.2(1)	−24.2(1)	−23.7(1)

b.d.l. = below detection limits, n.d. = not determined.

A secondary source of *n*-alkanes may be present, in addition to the waxes from terrestrial higher plants, with a C_{max} around C_{17} and no carbon preference, suggesting a microbial or algal contribution to the lignite (Philip, 1985; Killops and Killops, 2005; Peters *et al.*, 2005). These microorganisms usually do not require long-chain *n*-alkanes because most of these organisms reside in subterranean or aquatic environments.

The *n*-alkanone and *n*-alkanal distributions are not easy to decipher, due to their diversity of sources and origin. *n*-Alkanones have been reported to form as biotic constituents of higher plants (*e.g.* epicuticular waxes) and *Sphagnum* peat mosses, occurring *via* microbial or photochemical oxidation of *n*-alkanes, and to occur in hydrothermally altered organic matter (Eglinton and Hamilton, 1967; Lehtonen and Ketola, 1990; George and

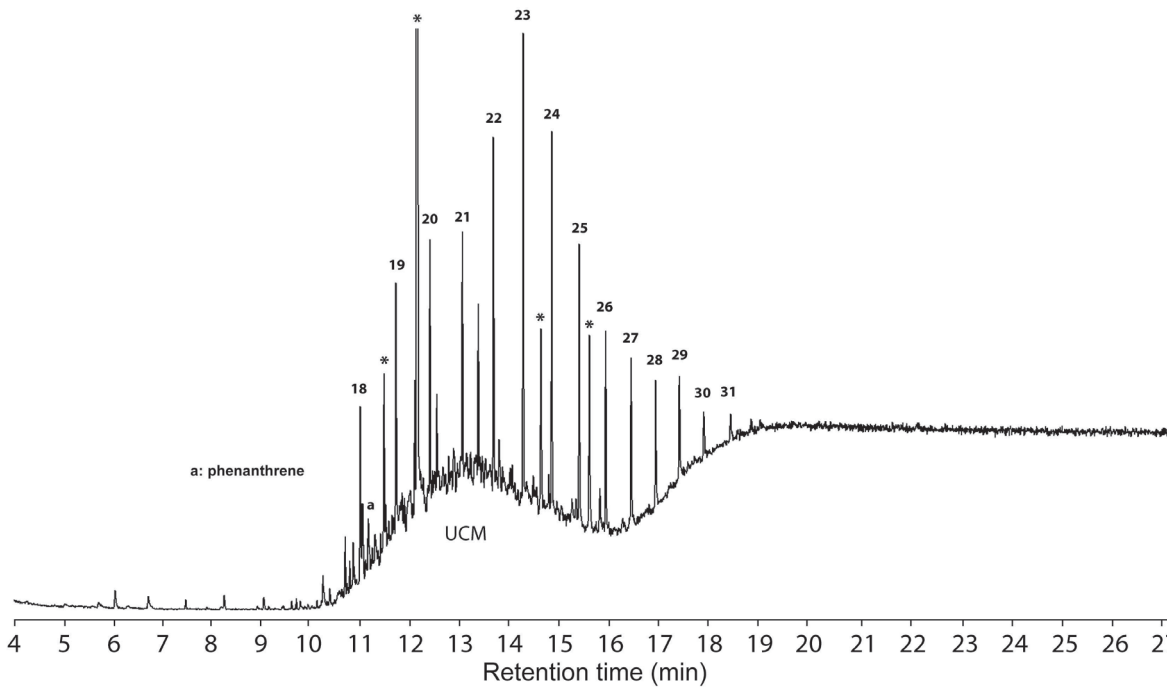

Figure 10. Total ion chromatograph of cs72508-8 extract. Peak numbers represent the carbon number for each *n*-alkane. UCM = unresolved complex mixture. * represents phthalate and silicone contamination.

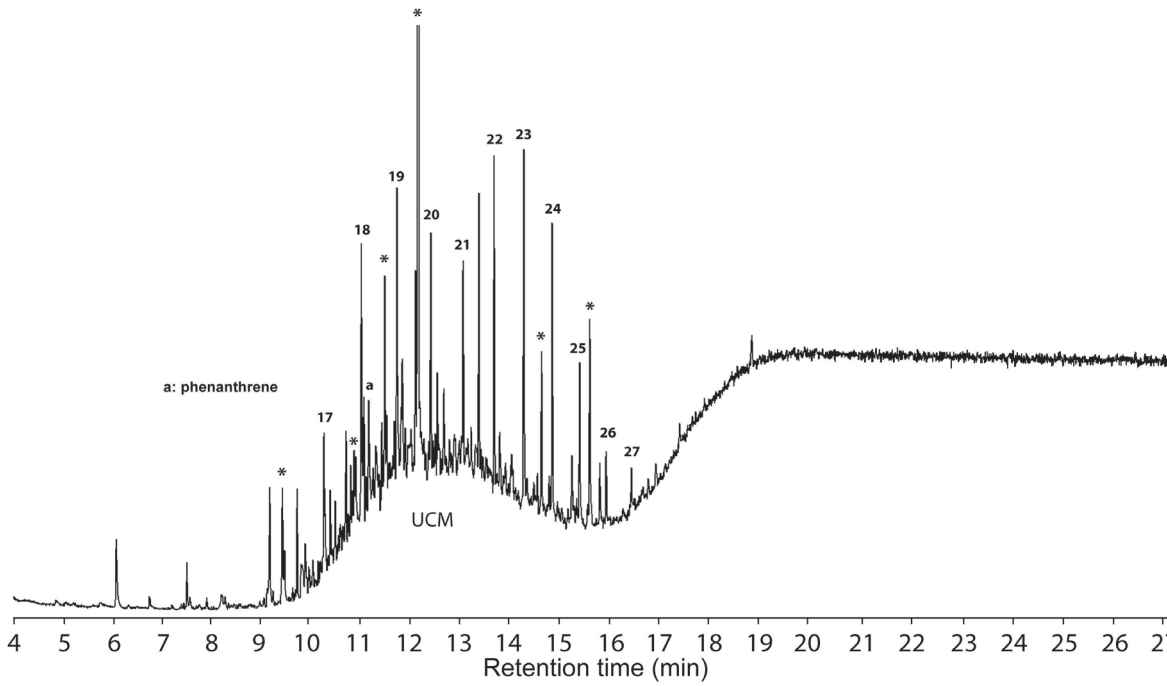

Figure 11. Total ion chromatograph of enn71908-3 extract. Peak numbers represent the carbon number for each *n*-alkane. UCM = unresolved complex mixture. * represents phthalate and silicone contamination.

Jardine, 1994; Leif and Simoneit, 1995; Baas *et al.*, 2000, Nichols and Huang, 2007). The similar chain-length distribution between the *n*-alkanones and *n*-alkanes, in addition to a similar odd-over-even preference and absence of steroidal constituents, points to the oxidation of epicuticular *n*-alkanes as a possible source of *n*-alkanones.

Similarities between the *n*-alkanes and *n*-alkan-2-ones do not clarify where oxidation of the *n*-alkanes occurred, however, *i.e.* on the leaf surface, during organic matter transport, or during diagenesis. Evidence indicates that a majority of the *n*-alkan-2-ones in sediment or at leaf surfaces have a microbial origin, from either β-oxidation of *n*-alkanes or β-oxidation and decarboxylation of *n*-alkanoic acids (Brassell *et al.*, 1980; Volkman *et al.*, 1980; Albaiges *et al.*, 1984; Grimalt *et al.*, 1991; Tuo and Li, 2005) (Figure 13). The greater concentration of *n*-alkan-3-one and *n*-alkan-4-ones associated with the kin72608 lignite could be interpreted as resulting from more significant microbial oxidation of the δ- and γ-carbon positions of the *n*-alkanes during diagenesis (Tuo and Li, 2005). The change in *n*-alkanone distribution may also be due to subaerial exposure of the kin72608 lignite in the open-pit mine, however, whereas the mc73108 lignite was from a horizon that was never exposed aerially by mining processes.

n-Alkanals have a mode of origin similar to the *n*-alkan-2-ones in the sedimentary record, where many are formed from photochemical and microbial α- and β-oxidation of *n*-alkanes (Schulte and Shock, 1993). Along with the discrepancies observed in the *n*-alkanone distribution between the two lignites, a significant difference in *n*-alkanal concentrations exists. *n*-Alkanals are usually diagenetically altered to *n*-alkanoic acids or *n*-alkanols, leaving sediments with a large *n*-alkanone/*n*-alkanal ratio (Prahl and Pinto, 1987; Lehtonen and Ketola, 1990; Nichols and Huang, 2007). In spite of the instability of *n*-alkanals during diagenesis, their preservation in the kin72608 lignites is noteworthy. The data suggest, therefore, that either the *n*-alkanals were preserved as a result of the geochemical conditions present in the kaolins or they were authigenic, resulting from atmospheric exposure from mining. *n*-Alkanals have been reported to undergo polymerization under alkaline conditions (Lamberton, 1965; Prahl and Pinto, 1987). Therefore, one may assume that *n*-alkanals are more stable under acidic conditions. The kaolins have pH values ranging from 3.5 to 6.5 (as a 5 wt.% aqueous slurry), possibly providing a stable environment for *n*-alkanals. Alternatively, opening of the kin72608 mine may have exposed the organic matter to a water-rich and oxic environment, potentially facilitating the formation of *n*-alkanal.

The lignitic kaolins generally show evidence for contributions from microbial lipids. The hopane homologues are diagenetic products of bacteriohopanetetrol, which is a lipid membrane modifier (Rohmer *et al.*, 1980). The dominance of αβ- and βα-hopane stereoisomers is typical of a peat-based environment, where αβ-C_{31}-hopanes were dominant, whereas other hopanes are dominant in sediments (Quirk *et al.*, 1984). The

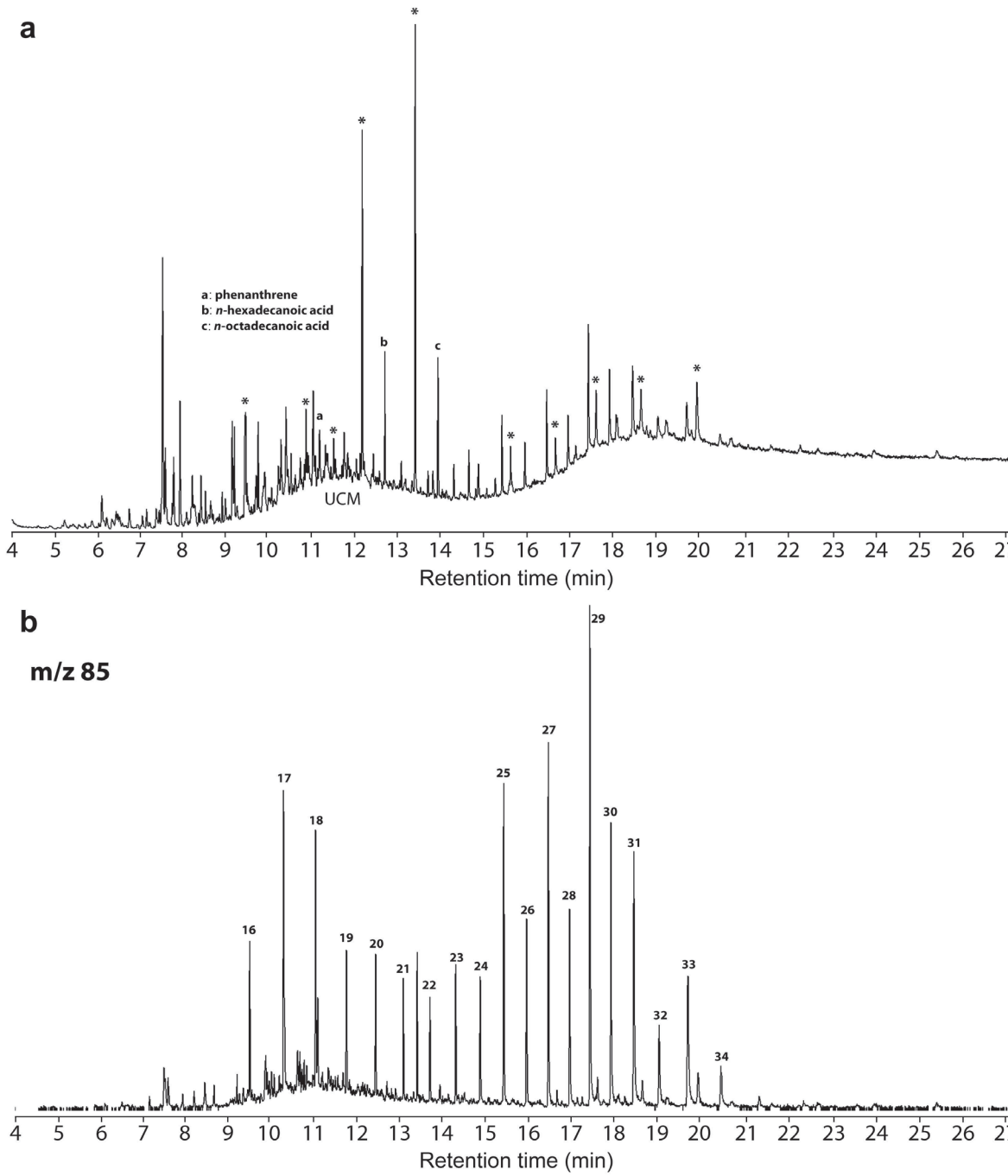

Figure 12. Total ion chromatograph and m/z 85 fragmentogram of rou62608-4. Peak numbers represent the carbon number for each *n*-alkane. UCM = unresolved complex mixture. * represents phthalate and silicone contamination.

hopane distributions in the lignitic kaolins from this study are unique because of the absence of $\Delta^{17(21)}$-hopenes and $\Delta^{13(18)}$-neohopenes (Quirk *et al.*, 1984; Brassell *et al.*, 1985). These hopenes typically coexist with hopanes in peats derived from mosses (Quirk *et al.*, 1984; Brassell *et al.*, 1985). A possible explanation for the lack of hopenes in these samples is their diagenetic alteration in the acidic environment facilitated by the Al-rich surfaces of the kaolinite. Kaolinite surfaces are known to be efficient Brønsted acids that can yield H^+ from pore waters, thereby potentially promoting hydrogenation of the $\Delta^{17(21)}$-hopenes and $\Delta^{13(18)}$-neohopenes. No direct evidence of hopene hydrogenation exists, however, although the compound-specific δ^2H characteristics of the hopanes and groundwater could be determined to verify whether H-exchange occurred

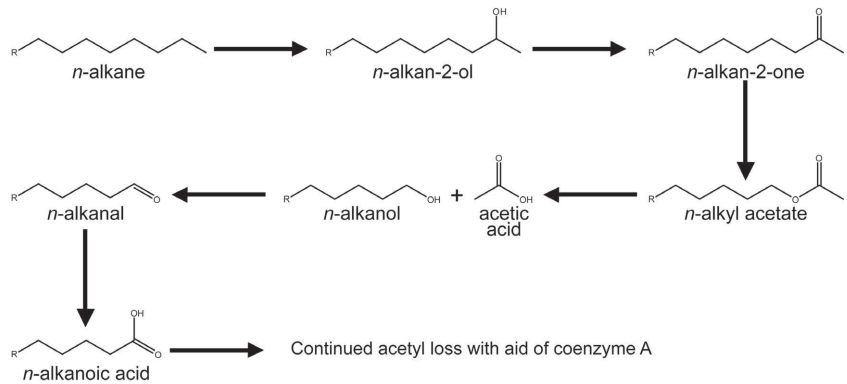

Figure 13. Aerobic oxidation of *n*-alkanes via the β-oxidation reaction pathway responsible for the formation the oxygenated *n*-alkyl lipids and organic acids (after Killops and Killops, 2005).

between the $H_{(hopane)}$ and $H_{(porewater)}$. In addition, compound-specific $\delta^{13}C_{(hopanes)}$ analyses would also be able to determine better the hopane source(s) (Freeman *et al.*, 1990). Lignitic sediments may also contain $\Delta^{17(21)}$-hopenes and $\Delta^{13(18)}$-neohopenes which were formed by a different microbial community than that producing the hopanoids in these lignites.

A comparison of homologue relative abundances demonstrates that the mc73108 hopanoids are more altered than the kin72608 lignites. The mc73108 lignite has a greater abundance of the C_{27}- and C_{28}-hopane homologues, whereas the kin72608 lignite is dominated by the C_{31}- and C_{32}-hopanes. Hydroxyl groups are lost and the 17-C alkyl chain becomes shortened from the C_{35}-hopanes to C_{27}-hopanes under diagenetic conditions. Extending down the smaller hopanoid homologues is the occurrence of the 17,21-secohopanes in the mc73108 lignite (17,21-secohopanes were absent in the kin72508 lignite). These secohopanes have been attributed to microbial opening of the ring E of hopanoids during early diagenesis (Trendel *et al.*, 1982). Oxidation of $\Delta^{17(21)}$-hopenes followed by reduction to the 17,21-secohopane homologues was described by Trendel *et al.* (1982) as a potential mechanism for the formation of 17,21-secohopanes from the hopane series.

The lignitic kaolin biomarker data demonstrate that differing mechanisms drove the diagenetic alteration of organic matter. Oxidation and gradual decomposition of the detrital organic matter is evident, however, in all samples evaluated in this study. Continual oxidation and decomposition of the organic matter in the lignitic kaolins would have removed any biological signatures and produced high functionalized organic constituents that would influence the mineralogical and industrial properties.

Lean kaolin

Biomarker analyses are not appropriate for the lean kaolins: few preserved biomarkers exist in these samples. The lean kaolins were dominated by unresolved complex mixtures (UCM) of hydrocarbons that are related to either petroleum contamination or extreme biodegradation (Brassell and Eglinton, 1980). The UCM in these kaolins is more likely to arise from biodegradation, based on hopane distribution in the lignitic kaolins and ^{13}C enrichment with decreasing organic carbon concentrations. The UCM cannot be characterized using traditional GC-MS techniques due to the unresolved nature of the material. A majority of UCM was found (Gough and Rowland, 1990) to be composed of monoalkyl-substituted T-branched alkanes, because microorganisms cannot efficiently degrade the organic matter at the T-branch site. The presence of UCM is the strongest indicator of extensive microbial biodegradation of the indigenous organic matter in the Georgia kaolins.

The resolvable constituents within the lean kaolins are dominated by C_{16} to C_{23} *n*-alkanes with no odd or even chain-length preference and C_{16} and C_{18} *n*-alkanoic acids. These organic constituents are typical of microorganism (bacteria/cyanobacteria, algae) lipids (Philps, 1985; Killops and Killops, 2005; Peters *et al.*, 2005). Dongwei *et al.* (2010) reported that algal C_{16} to C_{23} *n*-alkanes degrade rapidly in the presence of kaolinite, independent of the redox conditions. Therefore, the presence of C_{15} to C_{22} *n*-alkanes in the kaolins suggests that the microorganisms were still present at the time of collection and possibly extraction. Low abundances of pristane or phytane in these samples indicate that *n*-alkanes were not derived from photoautotrophs such as algae and cyanobacteria, but rather from bacteria. Microbiological studies have identified evidence for the occurrence of microorganisms in the kaolin lenses (Barker and Hurst, 1992; Shelobolina *et al.*, 2005; 2007). These studies provide evidence for a wide variety of microorganisms that either are or have been present in the kaolin lenses, cycling much of the inorganic and organic constituents. The major microorganisms currently in the kaolin lenses are Fe^{2+}-oxidizing and Fe^{3+}-reducing bacteria, along with sulfate-reducing and methanogenic bacteria (Shelobolina *et al.*, 2005, 2007). Oxidation of organic matter is an essential step for

electron transfer in the Fe^{3+}- and SO_4^{2-}-reducing processes. The kaolins from these studies included various forms of organic matter as potential electron donors: formate (~30.6 mmol/kg), acetate (~40.5 mmol/kg), lactate (~12.1 mmol/kg), pyruvate (~78 mmol/kg), oxalate (~141.7 mmol/kg), and citrate (~1.4 mmol/kg) (Shelobolina *et al.*, 2005). These acids would have been generated *via* α- and β-oxidation of the detrital organic matter during both aerobic and anaerobic oxidation.

Although no usable biomarkers were found in the lean kaolins, many of these samples contained minor amounts of humic materials, *i.e.* humic acid, fulvic acid, and humin. The humic materials were observed in the extracted phase, but were neither quantified nor characterized. This aspect should be addressed in the future because of the significant influence humic materials can have on particle orientation, mineral crystallization, and metals distribution. Humic materials primarily develop from the decomposition of lignin, producing large, complex acids that have a high concentration of oxygen-based functional groups, *i.e.* carboxyl (COOH), phenolic (OH), alcoholic (OH), and methoxy (OCH_3). Due to their high concentrations of oxygen, humic substances have a strong affinity for clay-mineral surfaces and metals (Tombácz *et al.*, 2004; Killops and Killops, 2005). Humic materials, in addition to microbial siderophores, also have the potential to increase metal mobility *via* ligand-enhanced dissolution of Fe^{3+}- and Al^{3+}-bearing minerals (Sutheimer *et al.*, 1999; Maurice *et al.*, 2001; Rosenberg and Maurice, 2003). Extensive groundwater migration can transport these bound metals throughout the sediment until the chelating agent reaches conditions that cause metals to desorb. At this point, Al^{3+} and Fe^{3+} are released, potentially forming authigenic minerals, *e.g.* kaolinite recrystallization and Fe oxide crystallization.

SUMMARY AND CONCLUSIONS

Sources and diagenesis of the organic matter

Organic matter associated with the Georgia kaolins was mainly terrestrially derived, conifer plant material with significant contributions from microbial lipids and microbial oxidation of detrital OM or older microbial lipids. The lignite lenses appear to represent extended periods of increased rainfall resulting in the accumulation of organic debris and growth of peats in a waterlogged environment. In addition, different diagenetic redox conditions appear to have influenced lipid abundances and distributions within the lignite. In western Wilkinson County, lignite appears to have experienced more severe oxic weathering, indicated by a greater abundance and diversity of the oxygenated lipids in the lignite horizons. Conversely, evidence also exists for less oxic weathering (possibly as a result of less groundwater interaction or lower Eh weathering) of the organic matter, indicated by the lower abundance and diversity of oxygenated lipids in the lignites within Washington County.

As most of the original organic matter in the lean kaolins has been decomposed intensely, biomarker analyses could not be performed on the lean kaolins. However, the original organic matter constituents (not concentrations) of the lean Tertiary kaolins at the time of deposition may reasonably be assumed to be similar to those in the lignitic kaolins because the source area is not likely to have changed significantly (Dombrowski, 1993; Elzea Kogel *et al.*, 2002). Only minor changes were observed in the kaolin mineralogy and geochemistry above and below the lignite lenses, further supporting the idea of a restricted provenance during deposition of the Tertiary kaolins. Slight mineralogical changes associated with the Tertiary kaolins have been attributed primarily to diagenetic alterations (Schroeder *et al.*, 2004). Unfortunately, previous assumptions regarding the original organic matter characteristics cannot be applied to the Cretaceous kaolins as no lignites are associated with the Cretaceous kaolins evaluated in this study.

As the original composition of the kaolins was probably dominated by terrestrial plant and moss constituents, the unresolved complex material (UCM) and microbial lipids observed in the lean kaolin lenses are strong indicators that all of the original organic matter had been decomposed/oxidized. α- and β-oxidation of the original organic matter produced a wide range of functionalized organic constituents (*e.g. n*-alkanones, *n*-alkanals, and organic acids) as is shown by the lignitic kaolin composition and previous research (Shelobolina *et al.*, 2005, 2007). Decomposition of organic matter occurs primarily during early diagenesis when unconsolidated sediments are aerobically bioturbated, yielding an abundance of organic acids. The production of organic acids combined with the development of an anoxic environment facilitated the growth of anaerobic microorganisms, *e.g.* Fe-reducing, Fe-oxidizing, and SO_4-reducing bacteria. Organic acids probably had the most influence on the mineralogy and metal mobility, as both are susceptible to increased dissolution in the presence of organic acids.

Organic matter/mineralogy interaction

The kaolin-rich environment has potentially stabilized the *n*-alkanals and hydrogenated the $\Delta^{17(22)}$-hopene constituents. The clay-rich environment appears not to have facilitated the preservation of the organic matter, however. The low-temperature, water-rich environment may have catalyzed organic matter alteration and retarded preservation of the organic matter. The organic acids produced during the early aerobic oxidation should have had significant influence on the mineralogy and metals distribution (*e.g.* rare-earth elements, Fe, and Al).

The production of organic acids during aerobic oxidation that accompanied early diagenesis was prob-

ably one of the more important steps in the diagenetic reactions associated with these kaolin deposits. The low-temperature depositional environment of the kaolins suggests that many diagenetic reactions would be kinetically retarded in the absence of organic acids. Kaolinite dissolution, however, is enhanced in the presence of various organic acids and siderophores. The potential promotion of kaolinite dissolution during diagenesis would, in turn, promote the *in situ* recrystallization of kaolinite or formation of kaolinite overgrowths on detrital kaolinite particles. The greater degree of recrystallization observed in the Buffalo Creek Fm. kaolins compared with Jeffersonville Mbr. kaolins is partly related to the amount of organic acids present during diagenesis.

The presence of organic acids will also help to support the microbial populations that have been or are currently present in the kaolins (Shelobolina *et al.*, 2005, 2007). These microorganisms are believed to have had great influence on the iron and sulfur chemistries. Therefore, the presence of organic acids during deposition and diagenesis would have facilitated the formation or alteration of the iron (oxyhydr)oxides and iron sulfides that are common throughout the deposits. Iron (Shelobolina *et al.*, 2005, 2007) and sulfur (unpublished data) would appear to have undergone microbial reduction during diagenesis.

Many of the ideas relating organic acids to mineralogy and metals mobility are derived indirectly from organic matter evidence from the current study and from previous publications. To better address these concepts, however, further work is needed to examine the distribution of the organic acids and other organic ligand constituents (*e.g.* humic materials and siderophores) with respect to metal concentrations and particle morphology of the Georgia kaolins.

ACKNOWLEDGMENTS

The present study was funded partially by a student research grant from The Clay Minerals Society and by the Indiana University Grassmann Fellowship in Clay Mineralogy. Fieldsites were graciously opened to the authors by Imerys, Inc. Facilities offered by the Indiana University biogeochemistry laboratories are greatly appreciated. This manuscript was improved significantly by the reviews of and discussions with Drs Arndt Schimmelmann, Jessica Elzea Kogel, Lisa Pratt, Seth Young, and Haydn Murray. The authors thank the two anonymous reviewers.

REFERENCES

Albaiges, J., Algaba, J., and Grimalt, J. (1984) Extractable and bound neutral lipids in some lacustrine sediments. *Organic Geochemistry*, **6**, 223–236.

Baas, M., Pancost, R., van Geel, B., and Damsté, J.S. (2000) A comparative study of lipids in *Sphagnum* species. *Organic Geochemistry*, **31**, 535–541.

Barker, W.W. and Hurst, V.J. (1992) Bacterial trace fossils in Eocene kaolin of the Huber Formation of Georgia; *Phylloderma microsphaeroides*, n. ichnogen., n. ichnosp. *Ichnos*, **2**, 55–60.

Benner, R., Fogel, M.L., Sprague, E.K., and Hodson, R.E. (1987) Depletion of ^{13}C in lignin and its implications for stable carbon isotope studies. *Nature*, **329**, 708–710.

Blunt, J.W., Czochanska, Z., Sheppard, C.M., Weston, R.J., and Woolhouse, A.D. (1988) Isolation and structural characterization of isopimarane in some New Zealand seep oils. *Organic Geochemistry*, **12**, 479–486.

Brassell, S.C. and Eglington, G. (1980) Environmental chemistry – an interdisciplinary subject. Natural and pollutant organic compounds in contemporary aquatic environments. Pp. 1–22 in: *Analytical Techniques in Environmental Chemistry* (J. Albaiges, editor). Pergamon Press, Oxford, UK.

Brassell, S.C., Comet, P.A., Eglinton, G., Isaacson, P.J., McEvoy, J., Maxwell, J.R., Thomson, I.D., Tibbetts, P.J., and Volkman, J.K. (1980) The origin and fate of lipids in the Japan Trench. Pp. 375–392 in: *Advances in Organic Geochemistry* (A.G. Douglas and J.R. Maxwell, editors). Pergamon Press, Oxford, UK.

Brassell, S.C., McEvoy, J., Hoffman, C.F., Lamb, N.A., Peakman, T.M., and Maxwell, J.R. (1984) Isomerization, rearrangement and aromatization of steroids in distinguishing early stages of diagenesis. *Organic Geochemistry*, **6**, 11–23.

Brassell, S.C., Murchison, D.G., Mason, R., Durand, B., Eglinton, G., Comet, P.A., Curtis, C.D., Bada, J., and de Leeuw, J.W. (1985) Molecular changes in sediment lipids as indicators of systematic early diagenesis [and discussion]. *Philosophical Transactions of the Royal Society of London A*, **315**, 57–75.

Dombrowski, T. (1993) Theories of origin for the Georgia kaolin: a review. Pp. 79–97 in: *Kaolin Genesis and Utilization* (H.H. Murray, W. Bundy, and C. Harvey, editors). CMS Special Publication **1**, The Clay Minerals Society, Bloomington, Indiana, USA, 341 pp.

Dongwei, L., Qian, S., and Wang, X. (2010) Decomposition of algal lipids in clay-enriched marine sediment under oxic and anoxic conditions. *Chinese Journal of Oceanology and Limnology*, **28**, 131–143.

Eglinton, G. and Hamilton, R.J. (1967) Leaf epicuticular waxes. *Science*, **156**, 1322–1335.

Elzea Kogel, J., Pickering, S.M., Shelobolina, E., Chowns, T., Yuan, J., and Avant, D.M. (2002) *The Georgia Kaolins: Geology and Utilization*. Society of Mining, Metallurgy, and Exploration, Inc., Colorado, USA, 84 pp.

Faure, G. and Mensing, T.M. (2005) *Isotopes: Principles and Applications*, 3rd edition. Wiley, 897 pp.

Freeman, K.H., Hayes, J.M., Trendel, J.M., and Albrecht, P. (1990) Evidence from carbon isotope measurements for diverse origins of sedimentary hydrocarbons. *Nature*, **343**, 254–256.

George, S.C. and Jardine, D.R. (1994) Ketones in a Proterozoic dolerite sill. *Organic Geochemistry*, **21**, 829–839.

Gough, M.A. and Rowland, S.J. (1990) Characterization of unresolved complex mixtures of hydrocarbons in petroleum. *Nature*, **344**, 648–650.

Grimalt, J.O., Yruela, I., Saiz-Jimenez, C., Toja, J., de Leeuw, J.W., and Albaiges, J. (1991) Sedimentary lipid biogeochemistry of an hypereutrophic alkaline lagoon. *Geochimica et Cosmochimica Acta*, **55**, 2555–2577.

Hassanipak, A.A. and Eslinger, E. (1985) Mineralogy, crystallinity, $^{18}O/^{16}O$, and D/H of Georgia kaolins. *Clays and Clay Minerals*, **33**, 99–106.

Hostettler, F.D., Rapp, J.B., Kvenvolden, K.A., and Luoma, S.N. (1989) Organic markers as source discriminants and sediment transport indicators in south San Francisco Bay, California. *Geochimica et Cosmochimica Acta*, **53**, 1563–1576.

Hurst, V.J. and Pickering, S.M. (1997) Origin and classification of Coastal Plain kaolins, Southeastern USA, and the role of groundwater and microbial action. *Clays and Clay Minerals*, **45**, 274–285.

Kennedy, M.J., Pevear, D.R., and Hill, R.J. (2002) Mineral surface control of organic carbon in black shale. *Science*, **295**, 657–660.

Killops, S. and Killops, V. (2005) *Introduction to Organic Geochemistry*, 2nd edition. Blackwell Publishing, Oxford, UK, 393 pp.

Killops, S.D., Raine, J.I., Woolhouse, A.D., and Weston, R.J. (1995) Chemostratigraphic evidence of higher-plant evolution in the Taranaki Basin, New Zealand. *Organic Geochemistry*, **23**, 429–445.

Lamberton, J.A. (1965) The long-chain aldehydes of sugarcane wax. *Australian Journal of Chemistry*, **18**, 911–913.

Laszlo, P. (1987) Chemical reactions on clays. *Science*, **235**, 1473–1477.

Lehtonen, K. and Ketola, M. (1990) Occurrence of long-chain acyclic methyl ketones in *Sphagnum* and *Carex* peats of various degrees of humification. *Organic Geochemistry*, **15**, 275–280.

Leif, R.N. and Simoneit, B.R.T. (1995) Ketones in hydrothermal petroleums and sediment extracts from Guaymas Basin, Gulf of California. *Organic Geochemistry*, **23**, 889–904.

Maurice, P.A., Vierkorn, M.A., Hersman, L.E., and Fulghum, J.E. (2001) Dissolution of well and poorly ordered kaolinites by an aerobic bacterium. *Chemical Geology*, **180**, 81–97.

Nichols, J. and Huang, Y. (2007) C_{23}–C_{31} *n*-alkan-2-ones are biomarkers for the genus *Sphagnum* in freshwater peatlands. *Organic Geochemistry*, **38**, 1972–1976.

O'Leary, M.H. (1981) Carbon isotope fractionation in plants. *Phytochemistry*, **20**, 4, 553–567.

O'Leary, M.H. (1993) Biochemical basis of carbon isotope fractionation. Pp. 19–28 in: *Stable Isotopes and Plant Carbon-Water Relations* (J.R. Ehleringer, A.E. Hall, and G.D. Farquhar, editors). Academic Press, New York.

Otto A., Walther, H., and Püttmann, W. (1997) Sesqui- and diterpenoid biomarkers preserved in *Taxodium*-rich Oligocene oxbow lake clays, Weisselster basin, Germany. *Organic Geochemistry*, **26**, 105–115.

Over, D.J., Sprague, E.K., Culp, R.A., Pickering, S.M., and Wenner, D.B. (1987) Deposition of Georgia commercial kaolins in upper estuaries: indicated by organic carbon $^{13}C/^{12}C$. *Abstracts from the Annual Meeting of the Geological Society of America*, **19**, 2.

Peters, K.E., Walters, C.C., and Moldowan, J.M. (2005) *The Biomarker Guide, Volume 1: Biomarkers and Isotopes in the Environment and Human History*. Cambridge University Press, Cambridge, UK, 471 pp.

Philps, R.P. (1985) *Fossil Fuel Biomarkers: Application and Spectra*. Methods in Geochemistry and Geophysics, Series **23**. Elsevier, Amsterdam 294 pp.

Prahl, F.G. and Pinto, L.A. (1987) A geochemical study of long-chain n-aldehydes in Washington coastal sediment. *Geochimica et Cosmochimica Acta*, **51**, 1573–1582.

Quirk, M.M., Wardroper, A.M.K., Wheatley, R.E., and Maxwell, J.R. (1984) Extended hopanoids in peat environments. *Chemical Geology*, **42**, 25–43.

Rohmer, M., Dastillung, M., and Ourisson, G. (1980) Hopanoids from C_{30} to C_{35} in recent muds. *Naturwissenschaften*, **67**, 456–458.

Rosenberg, D.R. and Maurice, P.A. (2003) Siderophore adsorption to and dissolution of kaolinite at pH 3 to 7 and 22ºC. *Geochimica et Cosmochimica Acta*, **67**, 2, 223–229.

Scholefield, D. and Whitehurst, J.S. (1980) Organic geochemistry of some Georgia-South Carolina Clays: C_{19}–C_{28} isoprenoids and the possible presence of a sesterterpene-derived hydrocarbon. *Journal of the Chemical Society – Chemical Communications*, **4**, 135–136.

Schroeder, P.A., Pruett, R.J., and Melear, N.D. (2004) Crystal-chemical changes in an oxidative weathering front in a Georgia kaolin deposit. *Clays and Clay Minerals*, **52**, 211–220.

Schulte, M.D. and Shock, E.L. (1993) Aldehyde in hydrothermal solution: standard partial molal thermodynamic properties and relative stabilities at high temperatures and pressures. *Geochimica et Cosmochimica Acta*, **57**, 3835–3846.

Seifert, W.K. and Moldowan, J.M. (1978) Application of steranes, terpanes and monoaromatics to the maturation, migration and source of crude oils. *Geochimica et Cosmochimica Acta*, **42**, 77–95.

Shelobolina, E.S., Pickering, S.M., and Lovely, D.R. (2005) Fe-cycling bacteria from industrial clays mined in Georgia, USA. *Clays and Clay Minerals*, **53**, 580–586.

Shelobolina, E.S., Nevin, K.P., Blakeney-Hayward, J.D., Johnsen, C.V., Plaia, T.W., Krader, P., Woodard, T., Holmes, D.E., VanPraagh, C.G., and Lovely, D.R. (2007) *Geobacter pickeringii* sp. nov., *Geobacter argillaceous* sp. nov. and *Pelosinus fermentans* gen. nov., isolated from subsurface kaolin lenses. *International Journal of Systematic and Evolutionary Microbiology*, **57**, 126–135.

Silverberg, M. (1996) *Chemistry: The Molecular Nature of Matter and Change*. Mosby, St. Louis, Missouri, USA, 1062 pp.

Sprague, E.K., Over, D.J., Gize, A.P., Pickering, S.M., and Wenner, D.B. (1988) Apparent salinity of depositional environments of commercial sedimentary kaolinites, Georgia, by carbon isotope analysis (delta $^{13}C/^{12}C$). *Abstracts from the Annual Meeting of Geological Society of America*, **20**, 7, A174.

Sutheimer, S.H., Maurice, P.A., and Zhou, Q. (1999) Dissolution of well and poorly crystallized kaolinites: Al speciation and effects of surface characteristics. *American Mineralogist*, **84**, 620–628.

Sutton, P.A., Lewis, C.A., and Rowland, S.J. (2005) Isolation of individual hydrocarbons from the unresolved complex hydrocarbon mixture of a biodegraded crude oil using preparative capillary gas chromatography. *Organic Geochemistry*, **36**, 963–970.

Tombácz, E., Libor, Z., Illés, E., Majzik, A., and Klumpp, E. (2004) The role of reactive surface sites and complexation of humic acids in the interaction of clay mineral and iron oxide particles. *Organic Geochemistry*, **35**, 257–267.

Trendel, J.M., Restle, A., Connan, J., and Albrecht, P. (1982) Identification of a novel series of tetracyclic terpene hydrocarbons (C24–C27) in sediments and petroleums. *Journal of the Chemical Society – Chemical Communications*, **5**, 304–306.

Tuo, J. and Li, Q. (2005) Occurrence and distribution of long-chain acyclic ketones in immature coals. *Applied Geochemistry*, **20**, 553–568.

Volkman, J.K., Gillian, F.T., Johns, R.B., and Eglinton, G. (1980) Sources of neutral lipids in temperate intertidal sediment. *Geochimica et Cosmochimica Acta*, **45**, 1817–1828.

Vogel, J.C. (1993) Variability of carbon isotope fractionation during photosynthesis. Pp. 29–46 in: *Stable Isotopes and Plant Carbon-Water Relations* (J.R. Ehleringer, A.E. Hall, and G.D. Farquhar, editors). Academic Press, New York.

White, G.N., Dixon, J.B., Weaver, R.M., and Kunkle, A.C. (1991) Genesis and morphology of iron sulfides in gray kaolins. *Clays and Clay Minerals*, **39**, 70–76.

Zachos, J., Pagani, M., Sloan, J., Thomas, E., and Billups, K. (2001) Trends, rhythms, and aberrations in global climate 65 Ma to present. *Science*, **292**, 686–693.

(*Received 9 May 2012; revised 2 October 2012; Ms. 669; AE: H. He*)